DMD Fast Forward. Published on September 5, 2008 as doi:10.1124/dmd.108.022962

Manuscript DMD # 22962

Pharmacokinetics, distribution, metabolism and excretion of deferasirox and its iron complex in rats

Gerard JM Bruin, Thomas Faller, Hansjörg Wiegand, Alain Schweitzer, Hanspeter Nick, Josef Schneider, K.-Olaf Boernsen, Felix Waldmeier

Novartis Pharma AG, Drug Metabolism & Pharmacokinetics, Basel, Switzerland (G.B., T.F., H.W., A.S., H.N., K.-O.B., F.W., J.S.[1])

DMD Fast Forward. Published on September 5, 2008 as DOI: 10.1124/dmd.108.022962
This article has not been copyedited and formatted. The final version may differ from this version.

DMD #22962

Running title: Disposition of deferasirox in rats

Corresponding author: Dr. Felix Waldmeier
Novartis Pharma AG
Drug Metabolism & Pharmacokinetics
Novartis Campus, WSJ-210.4.20
CH-4056 Basel, Switzerland
email: felix.waldmeier@novartis.com

Number of words in *Abstract*: 240

Number of words in *Introduction*: 430

Number of words in *Discussion*: 1570

Number of references: 35

Number of text pages: 26

Number of tables: 6

Number of figures: 9

Abbreviations: ADME, Absorption, distribution, metabolism and excretion; AUC, area under the plasma concentration-time curve; COSY, Correlated Spectroscopy; CYP, Cytochrome P450; DAD-UV, ultraviolet diode array detector; DFO, deferoxamine; DMSO, dimethylsulfoxide; EDTA, ethylenediaminetetraacetic acid; HMBC, Heteronuclear multiple bond correlation; HPLC, high-performance liquid chromatography; HSQC, Heteronuclear single quantum coherence; iv, intravenous; LC–MS, Liquid chromatography–mass spectrometry; LOD, limit of detection; LOQ, quantification limit; LSC, liquid scintillation counting; Mrp2, multidrug-resistance protein 2; MRT, mean residence time; MS, mass spectrometry; NMR, nuclear magnetic resonance; PEG, polyethyleneglycol; po, peroral; QWBAL, quantitative whole body autoradioluminography; ROESY, rotating frame overhauser enhancement spectroscopy

.

Abstract

Deferasirox (Exjade®, ICL670, CGP72670) is an iron-chelating drug for oral treatment of transfusional iron-overload in patients suffering from β-thalassemia or sickle cell disease. The pharmacokinetics and disposition of deferasirox were investigated in rats. The animals received single intravenous (10 mg/kg) or oral (10 or 100 mg/kg) doses of ^{14}C radiolabeled deferasirox. Biological samples were analysed for radioactivity (LSC, QWBAL), for deferasirox and its iron complex (HPLC-UV), and for metabolites (HPLC with radiodetection, LC-MS, ^{1}H- and ^{13}C-NMR, and 2-dimensional NMR techniques). At least 75% of orally dosed deferasirox was absorbed. The oral bioavailability was 26% at 10 mg/kg dose, and showed an over-proportional increase at the 100 mg/kg dose, probably due to saturation of elimination processes. Deferasirox-related radioactivity was distributed mainly to blood, excretory organs and GI-tract. Enterohepatic recirculation of deferasirox was observed. No retention occurred in any tissue. The placental barrier was passed to a low extent. Approximately 3% of the dose was transferred into the breast milk. Excretion of deferasirox and metabolites was rapid and complete within 7 days. Key clearance processes were hepatic metabolism and biliary elimination via Mrp2. Deferasirox, iron complex and metabolites were excreted largely via bile and feces (total ≥90%). Metabolism included glucuronidation at the carboxylate group (acyl glucuronide M3) and at phenolic hydroxy groups, as well as, to a lower degree, CYP-catalysed hydroxylations. Two hydroxylated metabolites (M1, M2) were administered to rats and were shown not to contribute substantially to iron elimination in vivo.

Introduction

As humans are unable to actively remove iron from the body, a clinically relevant state can occur if toxic levels of iron accumulate. This can occur as a result of repeated blood transfusions (as required in patients with β-thalassemia major or sickle cell disease), or due to excessive dietary iron uptake in patients with chronic anemias and hereditary hemochromatosis. Excess iron is deposited in the form of hemosiderin (insoluble 'iron cores' of degraded or partially degraded ferritin), primarily in the liver, spleen, several endocrine organs and the myocardium (Gabutti and Piga, 1996; Olivieri, 1999). If untreated, the gradual accumulation of iron leads to progressive organ dysfunction and ultimately, death (Olivieri and Brittenham, 1997).

Iron-chelating agents are thought to slowly mobilize iron by continuous binding of labile iron present in a 'transit pool', which is in equilibrium with the insoluble iron deposits. The iron chelate is then excreted in the urine and / or feces. More than 40 years of clinical experience with deferoxamine (DFO, Desferal®) has clearly established the clear therapeutic benefit of iron chelation, i.e. forced elimination of iron. For patients with β-thalassemia, the introduction of chelation therapy with DFO was life-saving as treatment was shown to reduce iron-related morbidity and to improve quality of life (Brittenham *et al*, 1994; Gabutti and Piga, 1996). Similar therapeutic benefits have also been documented for patients with sickle cell disease requiring regular transfusions (Cohen and Martin, 2001). However, the short plasma half-life of DFO and its poor oral bioavailability necessitates slow subcutaneous infusions with a pump over 8-12 hours for 5-7 days life long. This very demanding procedure is associated with poor compliance (Olivieri and Brittenham, 1997). Indeed, compliance has been shown to be absolutely crucial to obtain the full benefit offered by iron chelation (Gabutti and Piga, 1996).

Deferasirox (Exjade®, ICL670) is a novel once-daily, oral iron chelator designed to treat chronic iron overload in patients with transfusion-dependent anemias (Steinhauser *et al*, 2004). Due to its convenient oral administration, deferasirox is likely to facilitate compliance. The oral regimen of deferasirox is also likely to be more practical in less-developed countries.

DMD Fast Forward. Published on September 5, 2008 as DOI: 10.1124/dmd.108.022962
This article has not been copyedited and formatted. The final version may differ from this version.

For a good understanding of the disposition of deferasirox in man, which will be described in a separate paper, a thorough investigation of the processes involved in the disposition in rats was considered to be essential. In this report we describe the absorption, distribution, pharmacokinetics, metabolism (including chemical structures of metabolites), enterohepatic circulation and excretion of [^{14}C]deferasirox in rats, following iv and po administration. Furthermore, the kinetics and disposition of the iron complex of deferasirox [Fe(deferasirox)$_2$] was investigated after iv dosing.

DMD Fast Forward. Published on September 5, 2008 as DOI: 10.1124/dmd.108.022962
This article has not been copyedited and formatted. The final version may differ from this version.

Material and methods

Chemicals and reagents. Deferasirox (4-[3,5-bis-(2-hydroxy-phenyl)-[1,2,4]triazol-1-yl]-benzoic acid, $C_{21}H_{15}N_3O_4$, molecular weight 373.4, Figure 1a) was obtained from Novartis (Basel, Switzerland). Deferasirox radiolabeled with ^{14}C in positions 3 and 5 was prepared by the Isotope Laboratory of Novartis. The specific total radiolabeled components of the used batches ranged from 0.036 to 5.1 MBq/mg and the radiochemical purity was higher than 97%. ^{14}C-labeled Fe(deferasirox)$_2$ complex (molecular weight: 865.5, Figure 1b), with a specific radioactivity of 1.7 MBq/mg and a radiochemical purity higher than 98%, was also obtained from the Isotope Laboratory. For comparison with metabolites, the following reference compounds (deferasirox derivatives) were synthesized by the Novartis Institutes for BioMedical Research: 5-OH (M1); 3-OH (M2); 5'-OH (M4); 3'-OH (M5).

A crude enzyme mix from *helix pomatia*, containing β-glucuronidases and arylsulfatases, was purchased from Roche Diagnostics, Mannheim, Germany.

Other chemicals and reagents were of analytical grade.

Animals studies. Male pigmented Long Evans rats (205–260 g) were used for distribution studies, male albino Hanover–Wistar rats (185–320 g) were used for absorption, pharmacokinetics, distribution, biliary excretion, and enterohepatic circulation studies and female albino Hanover–Wistar rats (195–405 g), were used for galactogenic transfer, placental transfer, and distribution studies in sucking pups. The rats were purchased from Charles River Laboratories, Sulzfeld, Germany. TR$^-$ rats (strain: HsdAmc:TR-*Abcc*^{2}, 263-340 g, Harlan, Horst, The Netherlands), lacking the Mrp2 transporter, were used in a study to investigate the role of the Mrp2 transporter in the disposition of deferasirox .

Rats used for studies of absorption, metabolism and excretion were housed individually for up to 1 week in glass metabolism cages designed to quantitatively separate urine and feces. For distribution studies, rats were housed individually in type IV, standard cages. Apart from bile duct-cannulated rats that received Ringer® solution (Oxoid LTD, Basingstoke, Hampshire, England) instead of water, the rats had free access to standard food (NAFAG pellets 890, Provimi Kliba SA, Switzerland) and tap water prior to dosing and during the experimentation period.

DMD Fast Forward. Published on September 5, 2008 as DOI: 10.1124/dmd.108.022962
This article has not been copyedited and formatted. The final version may differ from this version.

All animal studies complied with Swiss animal welfare regulations and followed approved protocols.

Formulation. For iv administration of [^{14}C]deferasirox (10 mg/kg) into the tail vein, the compound was dissolved in PEG 400 and diluted with 5% aqueous glucose solution. The resulting ratio of PEG 400:glucose solution was 1:4. The final concentration of the dose solution was 5 mg/g. A similar formulation was used for the intravenous administration of the metabolites M1 and M2. For po dosing (by gavage) of [^{14}C]deferasirox 10 or 100 mg/kg, the compound was suspended in 0.5% aqueous Klucel HF, resulting in compound concentrations of 1 mg/g or 10 mg/g, respectively. For iv administration of [^{14}C]Fe(deferasirox)$_2$-complex (10 mg/kg), the vehicle was 0.9% sodium chloride solution resulting in a final concentration of 5 mg/g.

Assessment of absorption, distribution, metabolism and excretion. The ADME studies included investigation of the excretion balance, the kinetics in blood and plasma as well as the distribution pattern and the metabolism. Samples were collected up to 7 days after iv (10 mg/kg) and po (10 and 100 mg/kg) administration of [^{14}C]deferasirox and for up to 4 days (distribution up to 7 days) post dose after iv administration of the iron complex [^{14}C]Fe(deferasirox)$_2$ (10 mg/kg). Three rats from each dosing group were used except for the distribution studies, where one rat per time point was assessed. Radioactivity was determined by liquid scintillation counting (LSC) of biological samples (blood, plasma, urine, bile, feces, organs/tissues, carcass) using a Tri-Carb 2700 TR (PerkinElmer).

Urine and feces were collected quantitatively (urine on ice) at daily intervals up to 7 days post dose and were stored at –20°C until further analysis. For the investigation of kinetics in blood and plasma, venous blood (0.2-0.3 mL) was collected sublingually into heparin-containing tubes. During the sample collection, the rats were anaesthetized by inhalation of an oxygen/isoflurane mixture (97/3, v/v). Plasma was prepared immediately after blood collection by centrifugation at 2100 rpm for 10 minutes and stored at –20°C until further analysis.

The tissue distribution of total radiolabeled components in male rats in the ADME study, in female pregnant rats, lactating rats and sucking pups was investigated using QWBAL

DMD Fast Forward. Published on September 5, 2008 as DOI: 10.1124/dmd.108.022962
This article has not been copyedited and formatted. The final version may differ from this version.

(Hamaoka, 1990; Johnston *et al.*, 1990; Miyahara, 1989; Shionoya, 1992; Shigematsu, 1992; Ullberg, 1977). The sacrificed animals were immediately deep frozen in a mixture of dry-ice and hexane at –75^{o}C, rapidly shaven and embedded in a 2% pre cooled semi-liquid gel of sodium carboxymethyl-cellulose. This rapid freezing procedure was designed to avoiding any post-mortem diffusion of radioactive material in the body. Sagittal sections of 40 µm thickness were obtained at –20^{o}C in a CM 3600 PLC cryomicrotome (Leica MicroSystems GmbH, Nussloch, Germany) according to the method of Ullberg (1977). Following 48–60 hours of dehydration at –23^{o}C, the sections were exposed to Fuji BASIII Imaging plates (Fuji Photo Film Co. Ltd, Tokyo, Japan) for 1 day at room temperature in a lead shielded box in order to minimize the background noise signal. The duration of the exposure was chosen to allow detection of approximately 2 dpm/mg, *i.e.* the concentration corresponding to <1% of the radioactive dose if the radioactivity was evenly distributed throughout the body. The imaging plates were left for 3-4 minutes at room temperature in the dark and subsequently transferred to a Fuji BAS 2000 TR phosphor imager (Fuji Photo Film Co., Ltd., Tokyo, Japan) to be scanned at a 100 µm with a 1024 gradation. The tissue concentrations of total radiolabeled components were determined by comparative densitometry using one standard curve for each imaging plate. The results were processed using a MCID/M4 (3.0 Rev. 1.3) image analyzer (Imaging Research, St. Catherines, Ontario, Canada) and automatically converted into concentrations of total radiolabeled components using a linear calibration curve obtained from a radioactive blood scale processed under the same conditions as the samples (Schweitzer *et al.*, 1987). For reporting, selected sections were re-exposed for 1 day at room temperature in a lead shielding box onto SR screens and scanned at a 600 dpi (42 µm) in a Cyclone® PhosphorImager (Perkin Elmer). The image files were processed using Adobe Photoshop software. The limit of detection ((LOD after po administration, 100 mg/kg: 0.35 µg-eq/g; LOD other studies: 0.007 to 0.07 µg-eq/g) was defined as the mean of background (n=10) plus three standard deviations, and the limit of quantification (LOQ) was taken as three times the LOD.

Evaluation in pregnant and lactating rats. The placental transfer in pregnant rats was studied 1, 2, 8 and 24 hours after po administration of [^{14}C]deferasirox (30 mg/kg) on

Day 13 and Day 17 of gestation by means of LSC (samples from Day 13) or QWBAL (samples from Day 17). The tissues of the dams, the complete fetuses, placentas, amnion (Day 17 only) and amniotic fluid (Day 17 only) were analyzed in two dams per time point (1, 2, 8 and 24 hours), one animal at Day 13 and the other at Day 17.

The galactogenic transfer was investigated in lactating rats after po dosing of [^{14}C]deferasirox (10 mg/kg). The concentrations of total radiolabeled components and metabolite patterns were analyzed in breast milk and plasma up to 72 hours post dose. For sample collection a sparse modus was applied using eight rats (four pups per dam). At each time point plasma and milk was collected from four rats. Samples were taken at 0.5, 4, 24, and 72 h in group 1 and at 2, 8 and 48 h in group 2. To estimate the amount of compound excreted into milk during a collection period, the milk concentration was multiplied by the milk volume produced during that time period (daily milk production: 15 mL, Harkness 2001).

The distribution in sucking pups was investigated by QWBAL at 1, 2, 3, 4, 6, 8, 12 and 24 hours after po dosing of [^{14}C]deferasirox (10 mg/kg) to the dams. Four dams were dosed and each dam was kept together with eight pups. At each time point, one pup from each dam was investigated.

Biliary excretion. Bile was quantitatively collected on ice from the bile duct-cannulated rats (n=3) up to 72 hours after po administration of [^{14}C]deferasirox (10 mg/kg). Radioactivity was determined in bile, urine and feces. Additionally, the metabolite patterns in bile were investigated. For this study, the bile duct of the rats was double-cannulated under anesthesia (isoflurane) according to Rath and Hutchison (1989). A recovery phase of approximately 48 hours was established between surgery and dosing. During this recovery phase, bile was collected. In turn, synthetic bile comprising 25 mmol of sodium taurocholate, 0.3 mmol of 5-cholesten-3β-ol and 12.5 mmol of lecithin (3-*sn*-phosphatidylcholine from egg yolk) per liter of 0.9% sodium chloride solution, was continuously infused into the duodenum with a flow rate of 1 mL/h. Furthermore, 0.01 to 0.05 mg/kg buprenorphine (Temgesic®) was administered subcutaneously before the start of surgery and during the recovery phase for postoperative analgesia.

DMD Fast Forward. Published on September 5, 2008 as DOI: 10.1124/dmd.108.022962
This article has not been copyedited and formatted. The final version may differ from this version.

Enterohepatic circulation. Two groups of male rats were bile duct-cannulated as described above. To Group 1, donor rats (n=3), [^{14}C]deferasirox (12 mg/kg) was administered iv (vena femoralis). Bile was collected on ice individually for the time period 0–24 hours post dose. For the sampling period, synthetic bile was supplemented intraduodenally (1 mL/hour). In Group 2, one third of the pooled bile collected from Group 1 was infused into the duodenum of receiver rats (n=2) within 24 hours at a flow rate of 0.65 mL/h/rat. Following this period, synthetic bile was infused into the duodenum (1 mL/h) for the next 24 hours. Bile (on ice), urine (on ice) and feces were collected individually and quantitatively in 0–24 and 24–48 hour fractions. Radioactivity was determined in all fractions and additionally in the gastrointestinal tract, carcass and cage wash at the end of the study by LSC. The metabolite patterns were investigated in the bile of each rat. To calculate the absorption of deferasirox-related compounds, the sum of radioactivity recovered in bile, urine, and carcass (Group 2 rats) was divided by the radioactivity administered into the duodenum. The extent of enterohepatic circulation of deferasirox-related compounds after iv administration was calculated as follows: percent of radioactivity excreted with bile (Group 1 rats, iv, 0–24 hours) was multiplied by radioactivity absorbed in percent (Group 2 rats, after infusion into the duodenum), divided by 100.

Iron excretion. In a supplementary iron excretion study, 50 mg/kg of non-radiolabeled deferasirox or its metabolites M1 and M2 were administered intravenously to three bile duct-cannulated rats. The amount of iron excreted through urine and bile (0–24 hours) was analyzed.

Analysis of deferasirox and iron complex. Deferasirox and Fe(deferasirox)$_2$ were determined in plasma and urine using validated HPLC–UV (Rouan *et al*, 2001) or HPLC–MS/MS methods (unpublished) based on similar HPLC-systems. The LC–MS/MS system comprised a Series 200 HPLC setup (PerkinElmer, Waltham, MA) with an API3000 mass spectrometer (Applied Biosystems, Foster City, CA) with the ion source operated in the positive ion mode, the capillary temperature at 270°C and the spray voltage at 5 kV. Deferasirox and Fe(deferasirox)$_2$ were measured and quantified separately. In the ADME study with [^{14}C]deferasirox using Hanover-Wistar rats, the

HPLC-UV method was used for the quantitation of deferasirox and the iron complex in plasma, whereas the LC-MS/MS method was applied in the ADME studies with [^{14}C]Fe(deferasirox)$_2$ complex and [^{14}C]deferasirox in TR$^-$ rats. The lower limit of quantification in plasma with the HPLC-UV method was 0.67 µmol/L (252 ng/mL) for deferasirox and 0.28 µmol/L (242 ng/mL) for the iron complex. The lower limit of quantification in plasma with the HPLC-MS-MS method was 0.67 µmol/L (252 ng/mL) for deferasirox and 0.31 µmol/L (268 ng/mL) for the iron complex.

Metabolite profiling. *Sample preparation*

Prior to HPLC analysis, plasma aliquots from three animals were pooled per time point, diluted with 2–3 volumes of HPLC start solvent, and centrifuged. Urine aliquots from 2–4 rats were pooled over 0–48 hours post dose, diluted 5- to 10-fold with HPLC start solvent, and centrifuged. Aliquots of feces homogenates from three rats were pooled over 0–48 hours and extracted with six volumes of acetonitrile during 30 minutes over a shaker. The contents were centrifuged and the supernatant was concentrated *in vacuo*. The extraction recovery of radioactivity was 86–95%. Bile aliquots from two rats were pooled over 0–48 hours post dose and diluted with 10 volumes of HPLC start solvent.

HPLC methods for metabolite profiling and radioactivity detection. Metabolites contained in processed sample aliquots were separated using a Jasco micro HPLC set up (Jasco, Tokyo, Japan). Chromatography was run on LiChrospher® 100-5 RP18 ec (particle size 5 µm, pore size 100 Å endcapped, 250 x 2 mm I.D., Machery-Nagel, Düren, Germany), with guard column (4 x 2 mm I.D., same adsorbent), at 25°C. A solvent gradient was formed from (A) 25 mM aqueous ammoniumformate with 2.5 mM EDTA (pH 5.5) / acetonitrile (99:1 v/v), and (B) acetonitrile, at a flow rate of 200 µL/min with the following characteristics: run time (min)/%A: 0/95, 10/90, 60/55, 65/5, 70/5. Aliquot volumes of 50–200 µL were injected. A Jasco DAD-UV detector MD-910 at 235 nm or 260 nm wavelength in combination with an on-line, flow-through 500 TR series radioactivity detector (PerkinElmer) with a 100 µl admixing cell were used. LSC-cocktail Flo-Scint A (PerkinElmer) was added at a flow rate of 0.6 mL/min. Recovery from HPLC was close to 100% for plasma, urine, bile and feces extract. For micropreparative purposes, 4 mm I.D. columns with Nucleosil 100-5, C18 HD (Macherey-Nagel, Düren) and a flow-through

radiomonitor 506 C-1 (Berthold, Wildbad, Germany) equipped with a YG 150 solid scintillator cell or with liquid scintillator admixture were used.

The LC–MS system comprised an Agilent 1100 HPLC setup (Agilent Technologies, Waldbronn, Germany) with a Finnigan Deca XP ion trap mass spectrometer (Thermo Electron Corp., San Jose, CA) and a radioactivity detector, 500 TR series (PerkinElmer). The chromatography system described above for metabolite profiling was used, except that the mobile phase contained no EDTA. MS was operated both in the positive and negative ion mode with the capillary temperature at 270°C, the spray voltage at 4.8 kV and –4.0 kV (for electrospray ionization in the positive and negative mode, respectively). The auxiliary gas and sheath gas flow rate were at 0 and 31 arbitrary units, respectively. In-source fragmentation was performed at 20, 45 and 70 V. Xcalibur^{TM} software, version 1.3 (Thermo Electron Corp.) was used for instrument control, data acquisition and data processing. Metabolites were identified based on their observed mass and fragments in (MS)MS experiments. The isotope pattern due to the presence of ^{14}C atoms facilitated the interpretation of signals from drug-related metabolites. In addition, reference substances of the hydroxylated metabolites M1, M2, M4, and M5 were synthesized. The synthesized metabolites were compared with those isolated from the biological samples to confirm their structure identification.

Alternatively, a QTOF MS (Micromass, Wythenshawe, Manchester, UK) was used with electrospray ionization in negative ion mode and with the following settings: capillary temperature 100°C, desolvation gas temperature 150°C, cone voltage 30, 60 or 90 V, collision energy 22–30V. HPLC was run with a solvent gradient formed from water and acetonitrile containing 0.1% TFA (v/v).

NMR spectroscopy. Metabolite M3 was isolated from bile samples. Serial HPLC chromatography of bile aliquots with the same HPLC column as described above for metabolite profiling but with a 4 mm I.D. bore, was used for collection of separated fractions. This was followed by a second HPLC purification step and provided metabolite M3. Feces samples were extracted with acetonitrile, and the extracts were subject to serial HPLC chromatography, yielding metabolites M1, M2, and M4, in amounts of 200–280 µg, and in high purity suitable for NMR spectroscopy. NMR spectroscopy of deferasirox and of purified metabolites was performed on a Bruker DRX-500 NMR spectrometer (Bruker Biospin AG, Fällanden, Switzerland), with a 5 mm broadband

DMD Fast Forward. Published on September 5, 2008 as DOI: 10.1124/dmd.108.022962
This article has not been copyedited and formatted. The final version may differ from this version.

inverse probe with z-gradient. Unambiguous assignment of all ^{1}H– and ^{13}C–NMR signals of deferasirox was a key prerequisite to metabolite structure elucidation. Typically, solutions of 5–30 mg deferasirox in 0.7 mL DMSO-d_6 were used in ^{1}H-NMR, ^{13}C-NMR, ^{1}H,^{1}H-COSY, ^{1}H,^{13}C-COSY and long range ^{1}H, ^{13}C-COSY measurements in 2.5 mm tubes in DMSO-d_6 at 27°C.

Based on their MS and ^{1}H–NMR spectra and in comparison to deferasirox, the chemical structures of metabolites M1, M2, M3 and M4 were identified, particularly with respect to the exact position of either the OH- or glucuronic acid substituents.

Metabolite profiles in bile after conjugate cleavage. In order to investigate the presence of an acylglucuronide, bile samples (400 µL) were treated with 1.6 mL buffer of pH 10 (30 mmol/L disodium tetraborate + 42 mmol/L sodium hydroxide) for 20h at 37°C. Then, an aliquot was acidified with formic acid to pH 3, and analysed by HPLC as described in the method for metabolite profiling. In parallel samples, the pH was adjusted with 1.6 mL buffer of pH 5.1 (0.82 mol/L acetic acid, 1.80 mol/L sodium acetate) and 40 µL of a β-glucuronidase/arylsulfatase mixture was added. Incubation was run at 37°C for 20h. After incubation, the sample was acidified with formic acid to pH 3, and analysed by HPLC.

Analysis of iron. Iron was analyzed in urine and bile employing a two-step analytical procedure. In the first step, the sample was digested, *i.e.* the sample matrix together with the iron complex(es) were completely degraded (mineralized) and dissolved by a wet-chemical oxidation process with nitric acid as oxidant at high temperatures in a microwave heated high-pressure autoclave. In the second step, iron ions were measured by inductively coupled plasma optical emission spectrometry using a PerkinElmer Optima 3000XL ICP-OES system. This method is a validated analytical procedure applicable to the determination of iron in various biological matrixes, such as urine, serum, blood etc. In urine, typically iron levels in the range between 100 µg/L and 6 mg/L can be quantitatively determined. In bile, a concentration range from 0.5 mg/L to 100 mg/L can be determined directly from the mineralized solutions.

Pharmacokinetic analysis. The concentrations of total radiolabeled components in plasma and tissues are given in µg-eq/mL or µg-eq/g based on the respective parent

compound [deferasirox or $Fe(deferasirox)_2$]. The converting factors into µmol/mL or µmol/g were 373.4 for deferasirox and 865.5 for $Fe(deferasirox)_2$. AUC (area under the plasma concentration-time curve) and AUMC (area under the first-moment curve of the plasma concentration-time curve) were calculated by the linear trapezoidal rule. The following parameters were calculated using the equations below:

a) CL (clearance) = $Dose_{iv}/AUC$

b) MRT (mean residence time) = AUMC/AUC

c) V_{ss} (volume of distribution at steady state) = CL•MRT

d) bioavailability of deferasirox (in %): $F= (AUC_{po}/Dose_{po}) \times (Dose_{iv}/AUC_{iv}) \times 100$

The po absorption was defined as the sum of the urinary and biliary excretion of total radiolabeled components after administering 10 mg/kg of [^{14}C]deferasirox to bile duct-cannulated rats. The *in vivo* blood distribution of total radiolabeled components was calculated by comparing the concentrations of total radiolabeled components in blood (C_b) to that in plasma (C_p) after iv and po administration, according to the formula [100-(C_p • (100-hematocrit)/C_b)].

Results

Pharmacokinetics. The PK parameters and the concentration-time curves of total radiolabeled components, deferasirox, and its complex, Fe(deferasirox)$_2$, are summarized in Table 1 and shown in Figure 2. After iv administration of [^{14}C]deferasirox (10 mg/kg), the concentrations of total radiolabeled components in plasma declined rapidly: 20% and 3% of the initial concentrations of total radiolabeled components (C_{5min} in plasma 23 µg-eq/mL) were observed at 2 and 8 hours post dosing, respectively. The lowest detectable concentration of total radiolabeled components was analyzed in the 48-hour plasma sample (0.019 µg-eq/mL). The concentrations of total radiolabeled components basically represented the combined concentrations of unchanged deferasirox and Fe(deferasirox)$_2$ in plasma, which was in line with the low amounts of metabolites seen in plasma in Hanover-Wistar rats. Considering the time range of 5 minutes to 4 hours, a half life of 0.7 hours was estimated for deferasirox A terminal elimination phase with a longer half life appears to follow but could not be characterized. The plasma clearance of 6.2 mL/min/kg, which corresponds to a blood clearance of 9.9 mL/min/kg, and the volume of distribution of 0.46 L/kg were low and moderate, respectively. The blood clearance represented 18% of the hepatic blood flow in rats (13.8 ml/min) (Davies and Morris,1993), which classifies deferasirox as a drug with a low to moderate extraction ratio.

After po administration of [^{14}C]deferasirox (10 mg/kg) to Hanover-Wistar rats, C_{max} of total radiolabeled components was observed in plasma at 0.5 hours (3.18 µg-eq/mL). Thereafter, the ^{14}C levels declined rapidly to 0.022 µg-eq/mL at 24 hours. With the multi-exponential elimination and the limited number of PK timepoints (see Figure 2b), it was not feasible to determine the elimination half lives accurately after po dosing. For the initial elimination phase, a half life of about 0.5 hour can be estimated. After po administration of [^{14}C]deferasirox (100 mg/kg), the course of the kinetics in plasma was different from that observed after the 10 mg/kg dose. A plateau of high concentrations of total radiolabeled components (50.8 to 56.4 µg-eq/mL) was observed between 1 and 8 hours. Thereafter, the concentrations of total radiolabeled components declined rapidly to 0.98 µg-eq/mL at 24 hours. The bioavailability of deferasirox after po dosing of 10 mg/kg was moderate (26%). Following po administration of the 100 mg/kg dose, the exposure to deferasirox was overproportional; the AUC was 106-fold higher after the

DMD Fast Forward. Published on September 5, 2008 as DOI: 10.1124/dmd.108.022962
This article has not been copyedited and formatted. The final version may differ from this version.

100 mg/kg dose than after the 10 mg/kg dose. Therefore the bioavailability could not be determined adequately for the high dose.

The combined concentrations of unchanged deferasirox and Fe(deferasirox)$_2$ in plasma of Hanover-Wistar after po dosing and iv administration were similar to the concentrations of total radiolabeled components. Independent of the route of administration, the deferasirox:Fe(deferasirox)$_2$ ratio in plasma declined with time from 56 to 3.8 (10 mg/kg iv, 0.083 to 4 hours), 14 to 1.7 (10 mg/kg po, 0.5 to 8 hours) and 79 to 23 (100 mg/kg po, 0.5 to 8 hours).

Irrespective of the administration route or dose, the radioactivity in blood, which represents predominantly deferasirox, was bound to erythrocytes to an extent of approximately 25%.

Based on the combined excretion data of bile and urine from rats dosed with 10 mg/kg [^{14}C]deferasirox, oral absorption was 75%. Comparison of the renal radioactivity excretion after iv administration of a 10 mg/kg dose (7.2%), and of a po 10 mg/kg dose (7.1%) versus that after a po 100 mg/kg dose (10.6%), suggest that the 100 mg/kg-dose was absorbed to a similar extent as the low doses. Note that no experiment in bile duct-cannulated rats was performed with the 100 mg/kg dose.

After iv administration of [^{14}C]Fe(deferasirox)$_2$ (10 mg/kg), the concentrations of total radiolabeled components in plasma declined more rapidly than after administration of deferasirox: 12, 0.8 and 0.02% of the initial ^{14}C concentrations (C_{5min} in plasma 91.7 µg-eq/mL) were observed at 1, 8 and 96 hours, respectively. Within the observation period (up to 2 hours post dose), the concentration of total radiolabeled components in plasma consisted mainly of the deferasirox–iron complex and deferasirox. Considering the time range of 5 minutes to 2 hours, a half life of approximately 0.4 hours was estimated for Fe(deferasirox)$_2$. The Fe(deferasirox)$_2$:deferasirox ratio changed in plasma dramatically between 5 minutes (25) and 2 (1.4) hours post dose. The concentrations of the complex decreased markedly between these time points (90.0 to 1.90 µg/mL), whilst the concentrations of deferasirox were similar between 5 minutes and 1 hour (about 1.5 µg/mL) and declined between 1 and 4 hours to roughly 8-fold lower levels.

Tissue distribution. The tissue distribution pattern was typical for an organic acidic compound. Irrespective of the dose the radioactivity was moderately distributed

DMD Fast Forward. Published on September 5, 2008 as DOI: 10.1124/dmd.108.022962
This article has not been copyedited and formatted. The final version may differ from this version.

throughout the body as indicated by concentrations of total radiolabeled components in most organs and tissues similar or lower to those in blood, except for organs and tissues involved in excretion processes.

In the albino animals, the maximum concentrations of total radiolabeled components in individual tissues following 10 and 100 mg/kg po doses of [^{14}C]deferasirox were observed at 4 hours post dose. At this time point, the highest concentrations of total radiolabeled components were found in the kidney cortex, liver and intestine (approximately 3–4.5 µg-eq/g and 235–280 µg-eq/g after administration of the 10 and 100 mg/kg doses, respectively). The concentrations of total radiolabeled components in the other tissues were close to or below LOQ. After po administration of both doses, the distribution patterns were similar at 4 and 8 hours post-dose, with individual tissue concentrations only slightly lower after 8 hours. Following po administration of the 100 mg/kg dose, the highest $AUC_{0–168h}$ was found in the brown fat, liver, kidney and skin, which were approximately 7.1- to 2.5-fold that of blood. A whole body autoradiogram of an albino rat is shown in Figure 3a.

In the pigmented rats, the distribution pattern was similar to that in albino rats and no uptake of radioactivity into the melanin-containing structures was observed.

At 5 min following iv dosing of [^{14}C]deferasirox (1 mg/kg, pigmented rat), the highest levels of total radiolabeled components were observed in the liver and kidney cortex (88.9 and 73.6 µg-eq/g) followed by the heart, lung, adrenal, salivary gland and blood (27-18 µg-eq/g) (Figure 3b). Total radiolabeled components were not quantifiable at 168 h after iv administration in one of the investigated tissues.

Following iv administration of [^{14}C]Fe(deferasirox)$_2$ (10 mg/kg) the tissue distribution of total radioactivity was primarily intravascular, which is in line with the low volume of distribution (Table 1). The highest exposure values of total radiolabeled components (estimated for up to 8 h post dose) were observed in bile, liver and, kidney substructures (cortex, medulla, pelvis), which were between 2 and 7 times greater than in blood (32 µg-eq/mL·h). At 168 hours, residual radioactive traces were detected in the kidney cortex, bone marrow, spleen, liver, and lung, amounting to 0.4% of the total dose.

Galactogenic transfer. Around 3.3% of the radioactivity administered was transferred to the breast milk of lactating rats within 72 hours after the po dose of [^{14}C]deferasirox

(10 mg/kg). The transfer of radioactivity into the milk was rapid and the highest concentration of total radiolabeled components in the milk was observed at 2 hours post dose (19.8 µg-eq/mL). The milk/plasma ratios of radioactivity were highest in the time range 2 to 24 h post dose (between 10 and 24). The apparent terminal half-life in milk was about 5 hours. In milk, about 80% of the recovered radioactivity corresponded to the parent compound.

In female lactating rats, as investigated in the tissue distribution study by QWBA, concentrations of total radiolabeled components in the mammary glands (0.078 µg-eq/g) at 24 h after po dosing (10 mg/kg) were similar to those in the liver and kidney medulla (Figure 3c) and approximately 3 times higher than in blood.

Absorption and distribution in sucking pups. The sucking pups were exposed to deferasirox and/or its metabolites for at least 24 hours after po administration of [^{14}C]deferasirox (10 mg/kg) to the dams. Concentrations of total radiolabeled components above LOQ (0.022 µg-eq/g) were detected in the kidney cortex, liver, lung, muscle, esophagus, skin and stomach content of the pups. C_{max} in pups was observed at 8 hours post dose in the liver and kidney cortex (approximately 0.56 µg-eq/mL), which is approximately 8 times lower than in the respective tissues of male rats after po administration at the same dose level. A whole body autoradiogram of a sucking pup is shown in Figure 3d.

Placental transfer. The placental transfer of deferasirox-related components into the fetuses after a 30 mg/kg po dose of [^{14}C]deferasirox was minimal, the concentrations of total radiolabeled components being at least 12-fold lower than in the blood for the respective dams, and up to 36-fold lower than those in the placenta. The radioactivity in the fetuses represented <0.005% of the administered dose and appeared to be distributed evenly. No radioactivity was detected in the amnion and amniotic fluid at all time points on day 17. A whole body autoradiogram of a pregnant rat on day 17 is shown in Figure 3e.

Assessment of metabolites. In radiochromatograms of plasma after intravenous dosing, the predominant component was unchanged [^{14}C]deferasirox, representing 81

DMD Fast Forward. Published on September 5, 2008 as DOI: 10.1124/dmd.108.022962
This article has not been copyedited and formatted. The final version may differ from this version.

% of the $AUC_{0–8h}$ of plasma radioactivity (Figure 4a). Under conditions of sample preparation and chromatography for metabolite patterns, the iron complex dissociated. The $Fe(deferasirox)_2$ complex could therefore not be measured by this analytical method, and the [^{14}C]deferasirox peak included drug substance that had been present in the form of the complex. Metabolite M3 represented 1% of the radioactivity $AUC_{0–8h}$.

The major route of elimination was through bile (69.3 % of the dose within 72 hours after po dosing; Table 3, Figure 4b). Similar metabolite patterns were observed in bile after po and iv dosing. The acylglucuronide (metabolite M3) was predominant. After 10 mg/kg po dosing, M3 accounted for 26.6% and parent drug for 7.7% of the dose. Furthermore, approximately 10 metabolite peaks were detected and each accounted for 0.1–7.4% of the dose (see Table 2). Treatment of bile with β-glucuronidase/arylsulfatase caused the disappearance of metabolites eluting in the retention time range between 28 and 40 minutes, with simultaneous formation primarily of the hydroxy metabolites M1, M2 and deferasirox. This indicates that these metabolites were largely glucuronide and/or sulfate conjugates. Therefore, the bulk of the absorbed dose fraction was eliminated in the form of phase II metabolites by hepatobiliary transport.

Under the analytical conditions, the iron complex could not be measured in the bile. Therefore, no conclusions could be drawn regarding the biliary excretion of the $Fe(deferasirox)_2$ complex. However, in a separate study in rats with 50 mg/kg deferasirox, 356 µg and 39 µg of iron was excreted through bile and urine, respectively, within 24 hours post dosing. This finding was an indirect evidence that the $Fe(deferasirox)_2$ complex was excreted through bile and urine.

The fecal excretion of radioactivity following po administration of 10 mg/kg [^{14}C]deferasirox to the bile duct-cannulated rats (0–72 hours) amounted to 21.5% of the dose, representing non-absorbed parent drug. The fecal excretion of radioactivity following iv administration of [^{14}C]deferasirox to Hanover-Wistar rats (0–168 hours) amounted to about 89.0% of the dose (Table 3). [^{14}C]deferasirox was the major compound in feces extracts both after iv and po dosing (see Table 2 and Figure 4c). Furthermore, hydroxylated metabolites M1, M2, M4 and M5 were detected. The total content of the metabolites represented 23% of the administered oral dose. The metabolite pattern in the feces differed from that in the bile. This is explained by

DMD Fast Forward. Published on September 5, 2008 as DOI: 10.1124/dmd.108.022962
This article has not been copyedited and formatted. The final version may differ from this version.

microbial enzymatic degradation of the biliary metabolites (conjugates) in the gut, which leads to liberation of deferasirox and of the main phase I metabolites.

A typical metabolite pattern in urine after iv dosing is shown in Figure 4d. After oral dosing, the sum of characterized conjugated metabolites (M3, M6, M7 M8, and M1) amounted to 3.0% of the administered dose. The most prominent metabolite M4 amounted to 1.9% of the dose (Table 2).

In some plasma chromatograms, a front peak (P3) was observed. To investigate the nature of P3, this peak was collected during HPLC analysis, evaporated to dryness, redissolved in buffer and re-injected into the same HPLC system. The resulting pattern showed a main peak at the retention time of [^{14}C]deferasirox. Therefore, P3 is considered to represent mainly protein-bound deferasirox. Metabolite P16, which was observed in plasma and urine, could not be identified.

Identification of chemical structures of metabolites*. Mass spectrometric data.* The mass spectrometric data for deferasirox and its metabolites, obtained by LC–MS, is shown in Table 4. The primary metabolites M1, M2, M4 and M5, were found to contain an additional hydroxy group. The benzoic acid part (–44, –120 amu) was unchanged for M1 and M4, thus the hydroxy group was attached to one of the phenol rings of deferasirox. In several metabolites, the presence of a glucuronic acid and/or sulfate moiety was clearly indicated by mass increments of 192/176 and 96 amu, respectively, as compared to deferasirox, and by the corresponding fragmentation (–176, –80). The main metabolite M3 showed a fragmentation sequence which indicated the presence of a glucuronic acid moiety (–176) attached to the carboxylate group (–44) of the benzoic acid part (–120). This structure was consistent with the chemical instability of M3 at alkaline pH, under which conditions deferasirox was liberated. Instability and cleavage at elevated pH is a common property of acyl glucuronides (Shipkova *et al*, 2003). Also, at neutral pH, rearrangement can occur in this type of compound by migration of the acyl substituent from the 1-O position in the glucuronic acid to 2-O, 3-O and 4-O positions. In LC–MS analyses, rearrangement product(s) with a molecular ion peak of 550 in the positive ion mode, which is the same as for M3, were detected as a slightly shifted peak M3'. M3 itself was stable in plasma, urine and bile samples at 0°C and -20°C in the dark. However, a decrease in the peak area of M3 with an accompanying increase of the peak area of M3' was observed with bile samples that were left at room temperature

overnight. The same molecular weights of M3 and M3', the small difference in HPLC retention time, and the formation of M3' with simultaneous disappearance of M3 at room temperature suggest that the rearrangements product(s) are due to acylmigration. It can be noted here that reanalysis of bile samples after storage at -20°C for more than one year reproduced the same metabolite pattern as depicted in Figure 4b, which demonstrated stability and very slow conversion to acyl migrated products.

NMR of deferasirox. The ^{1}H–NMR spectrum of deferasirox in DMSO-d_6 is shown in Figure 6a (signal range) and in Figure 6b (only aromatic region). A systematic numbering of the carbon atoms from C-1 to C-24 was used for NMR as shown in Figure 7. This numbering differed from the common chemical numbering used for deferasirox substructures (cf. Table 4 and Figure 8) but was introduced to unambiguously denote each C-atom position. The NMR data of deferasirox, including ^{13}C-shifts, ^{1}H-shifts, multiplicities, and homo- and heteronuclear correlations are tabulated in Table 6. A key requirement was the unambiguous assignment of the signal sets of the two phenolic ring systems (C 12–17 vs. C 18–23), attached to C-3 and C-5 of the triazole ring, respectively. According to Begtrup (Begtrup *et al*, 1988) and Schleucher (Schleucher *et al*, 1994), the ^{13}C NMR shifts of the C-3 atom in N-1-substituted 1,2,4-triazoles are shifted to low field as compared to the shift of the C-5 atom. Thus, in an HMBC experiment, the H-17 signal at 8.04 ppm (cf. Table 5 and Figure 6) was shown to correlate to the ^{13}C signal at 159.9 ppm (C-3 of triazole), and H-23 at 7.54 ppm correlated to the ^{13}C signal at 152.0 ppm (C-5 of triazole). Figure 7 shows the important COSY, ROESY and HMBC correlations in deferasirox used for the complete ^{1}H and ^{13}C signal assignment.

NMR of hydroxylated metabolites. The ^{1}H–NMR spectra of the purified metabolites M1, M2, and M4 were collected as for deferasirox. The spectral data are compiled in Table 6. The spectra of these three metabolites showed one additional exchangeable proton in comparison to deferasirox, verifying the existence of a third OH group indicated by MS. Correspondingly, one ^{1}H-signal for the site (C-atom) of OH-substitution was missing. Specific ^{1}H–NMR signals showing characteristic shifts as compared to deferasirox are indicated in Table 6 in bold font. For M1 and M2, the chemical shifts of H 20–23 and H-7/11 and H-8/10 comparable to deferasirox. For M4, the shifts of H 14–17 and H-7/11 and H-8/10 were comparable. Conversely, at the ring system where the OH

substituents were located, highfield shifts of the ^{1}H-signals were observed, and the multiplicities of the ^{1}H-signals in that ring were reduced. An OH group in an aromatic six-membered ring causes a strong highfield shift in ortho and para positions, but not in the meta position. M4 showed characteristic signal shifts analogous to those of M1, though in the phenol ring at triazole-C-5. Furthermore, meta coupling of "isolated" ^{1}H-signals (H-17 and H-23, respectively) ruled out other substitution patterns in M1 and M4. A different substitution pattern was seen in M2, with a characteristic triplet for H-16. With these considerations, it was possible to distinguish the non-compatible regio-isomers and identify the correct substituent positions. Thus, the sites of OH substitution in the metabolites could be assigned unambiguously. Further, the chemical structures of M1, M2 and M4 were confirmed by synthesis of reference materials which showed identical NMR and MS spectra. The structures are indicated in Table 4 and Figure 8.

NMR of metabolite M3. The ^{1}H–NMR spectrum of the glucuronide M3 was evaluated as above. The chemical shifts for H-20–23 and H-14–17 were essentially unchanged when compared to the ^{1}H signals of deferasirox. On the other hand, the ^{1}H-signals of H-8/10 shifted to a low field, demonstrating presence of the glucuronide at the carboxylate group of deferasirox. The ^{1}H shifts ar 5.62 and 3.85, denoted as H-1' and H-5' in table 6, respectively, could be clearly assigned to glucuronic acid proton signals. No evidence for acyl migration was observed.

Characterization of minor metabolites. LC–MS revealed that the minor metabolite, M6, was a direct glucuronic acid conjugate of deferasirox. It was shown to be identical to the M6 metabolite detected in urine from a mouse ADME study (results not shown here). The latter metabolite was analyzed using a LC–NMR approach similar to that described here. ^{1}H–NMR signals of M6 were largely unchanged compared with deferasirox except for H-14 and H-16, which showed a down-field shift of approximately 0.4 and 0.2 ppm, respectively. Therefore, M6 was identified as the 2-O-glucuronic acid conjugate of deferasirox. The minor metabolite, M5, was shown by LC–MS to be a hydroxylated metabolite different from M1, M2 and M4. Although, a sufficient amount for NMR could not be purified, it proved to be identical to a synthetic reference compound carrying the hydroxyl group in position "C-3" by comparison of HPLC retention times and MS data. In urine, the minor metabolites M7–M11 were found to be glucuronic acid or sulfate conjugates of hydroxylated metabolites. Incubation with glucuronidase or arylsufatase

DMD Fast Forward. Published on September 5, 2008 as DOI: 10.1124/dmd.108.022962
This article has not been copyedited and formatted. The final version may differ from this version.

enzyme preparations resulted in formation of metabolites M1, M2 and M5. It is highly likely, though not proven, that the glucuronic acid or sulfate moieties were attached to the additional hydroxy groups in the M1, M2 and M5 metabolites. Other minor metabolites, M12 and M13, were partly characterized. M12 was doubly conjugated, with both glucuronic acid and sulfate, while M13 was a sulfate conjugate, with sulfate linked at the 2-O or 2'-O position. Identification of metabolites across sample types was achieved based on HPLC rt, mass spectral properties and comparison with reference compounds.

Excretion. Excretion data in urine, bile and feces after administration of [^{14}C]deferasirox and [^{14}C]Fe(deferasirox)$_2$ are summarized in Table 3. Following iv (10 mg/kg) and po (10 or 100 mg/kg) doses of [^{14}C]deferasirox, excretion in urine and feces was complete (mean: 101% of the dose, n=9, CV 4%) within 7 days post dose. Excretion in urine was minor (6–11%). After a po administration of 10 mg/kg to bile duct-cannulated rats, 6.3, 69.3 and 21.5% of the dose was recovered in urine, bile and feces, respectively. After iv administration of 10 mg/kg [^{14}C]Fe(deferasirox)$_2$, the recovery of radioactivity in the excreta was very similar to that observed for deferasirox.

Enterohepatic circulation. After iv administration of 12 mg/kg [^{14}C]deferasirox to double bile duct-cannulated rats (Group 1, donor rats), the fraction of radioactivity excreted via bile was 82.6% (rat 1) and 73.7% (rat 2) within the 24 hour sampling interval, and 61.5% (rat 3) within the 6 hour sampling interval. In the bile pool of the three rats, the pattern of metabolites was similar to that shown in Figure 4b. Following the continuous intraduodenal infusion of the donor bile to the two receiver rats (Group 2 rats), within 24 hours post dose radioactivity was recovered in the bile (28.7%), urine (1.6%), feces (26.4%), gastrointestinal tract (20.9%), carcass (8.7%) and in cage wash (7.6%; mean values each). Accordingly, absorption of deferasirox-related compounds from the duodenum of the receiver rats amounted to 39%. The extent of enterohepatic circulation was calculated to be 30.5% of the iv administered dose, based on the biliary excretion of donor rats 1 and 2. Since the proportion of unchanged [^{14}C]deferasirox in the infused bile was only 12.5%, it was concluded that metabolites must have been reabsorbed as well. Conjugates of deferasirox in the bile of the donor rats may have

been cleaved in the gut, and liberated deferasirox may then have been reabsorbed. The metabolite pattern in the bile of the receiver rats was again similar to that in Figure 4b. However, slightly smaller proportions of metabolites were found.

Iron excretion. The potential contribution to chelation and elimination of iron of the primary hydroxylated metabolites M1 and M2 was assessed after intravenous administration of 10 mg/kg. Excretion of iron in bile and urine amounted to 62 µg per day for M1 and 70 µg per day for M2 and thus was substantially lower than that achieved with deferasirox (395 µg per day).

Disposition in Mrp2-deficient TR$^-$ rats. The role of the anion transporter Mrp2 in the disposition of deferasirox and its metabolites was investigated in TR$^-$ rats. This rat strain is deficient in the membrane transporter Mrp2 which catalyzes the hepatobiliary transport of conjugated bilirubin, glutathione conjugates and other organic anions including drugs and drug conjugates (Dietrich et al., 2001; Kim et al., 2003; Chan et al., 2004; Borst et al., 2006). Upon iv administration of 10 mg/kg [^{14}C]deferasirox, pharmacokinetics and disposition in the TR$^-$ rats differed markedly from those in Hanover-Wistar rats:

- The plasma concentrations of total radioactivity were far higher in TR$^-$ rats and decreased with a longer half-life (approx. 2 hrs, *vs* 0.7 hr) (Figure 2). The slower elimination of deferasirox-related radiolabeled material in TR$^-$ rats led to a 5-fold higher systemic exposure to ^{14}C components in TR$^-$ rats than in Hanover-Wistar rats. This indicated slower elimination processes with increased formation of metabolites.
- The biliary excretion of ^{14}C-radioactivity was reduced in TR$^-$ rats to 43% of the dose (vs. 69% in Hanover-Wistar rats) (Table 3). On the other hand, excretion of ^{14}C-radioactivity in urine was enhanced in TR$^-$ rats to 41% of the dose (vs. about 8%) (Table 3).
- The metabolite patterns in plasma, bile, feces and urine of TR$^-$ rats (Figure 4e-4h) showed much larger dose proportions in the form of metabolites. However, different types of metabolites were formed in the TR$^-$ rats: While in the bile of Wistar rats, the main metabolite M3 (acyl glucuronide) accounted for 27% of the dose (Table 2, Figure 4b), only a marginal amount of M3 was found in the bile of TR$^-$ rats (Figure 4f). On the

other hand, a different glucuronide (M9) and particularly several sulfate conjugates (M7, M8, M9, M12, M13) were the major or even the predominant metabolites formed. The latter metabolites were excreted with both urine and bile (Table 3).

- Unchanged deferasirox accounted for a smaller radioactivity proportion in plasma, bile, feces and urine (Figure 4e-4h), consistent with an increased extent of metabolism.

Discussion

An essential requirement for an efficacious oral iron-chelating drug is an optimal gastrointestinal absorption after oral dosing. The studies reported here demonstrate that deferasirox administered po to rats is absorbed to at least 75%, and the bioavailability was 26%. The difference between absorption and bioavailability following po administration was probably due to hepatic first pass elimination via bile.

After iv and po administration, deferasirox was present in the blood circulation mainly in the unchanged form and as its iron complex, Fe(deferasirox)$_2$. Deferasirox was 99.2% bound to plasma proteins. The iron complex had a smaller distribution volume than deferasirox, and the unbound fraction of the iron complex (0.3%) was smaller as compared with deferasirox (Weiss *et al*, 2006).

The volume of distribution of deferasirox was moderate. It was distributed throughout the body to a limited extent and for a short period of time, except in the kidney and liver. The liver is the key organ for elimination of deferasirox and its iron complex. In the liver, deferasirox binds iron, forming the Fe(deferasirox)$_2$ complex. The observed distribution pattern was typical for an organic acid compound, which is present as an anion at physiological pH. Deferasirox and the iron complex were eliminated rapidly from blood and the liver, largely via bile. Substantial concentrations of iron in bile and feces demonstrated the intended elimination of iron caused by deferasirox (Hershko *et al*, 2001; Nick *et al*, 2003).

Systemic elimination of deferasirox in the rat was mainly, but not exclusively, due to metabolism. The major metabolism pathways in the rat were direct glucuronidation that produced metabolites M3 and M6; hydroxylations at the phenol rings that resulted in metabolites M1, M2, M4 and M5; and conjugation of the hydroxylated metabolites with glucuronic acid and/or sulfate. It should be noted that at physiological pH, deferasirox and all its metabolites are mono- or di-anions. Similarly, the iron complex of deferasirox carries three negative charges. This suggests a major role for anion transport systems involved mainly in the hepatic uptake and hepato-biliary elimination process of deferasirox, as further discussed below. Similarly, the oxidative processes have been observed in *in vitro* studies of human hepatic microsomes. They are catalyzed mainly by human CYP1A1 and CYP1A2 enzymes resulting in metabolites M1 and M2, and to a lower degree by the human CYP2D6 producing metabolite M4 (Novartis data on file).

The main metabolite in the bile, M3, may retain the capability to form an iron complex, since glucuronic acid is attached to the molecule at a position distant from the complex-forming moiety. The metabolites M1 and M2 also retain the structural requirements to chelate iron. However, following iv administration of M1 and M2, comparatively low amounts of iron were eliminated. Therefore, after oral dosing of deferasirox the metabolites M1 and M2 will minimally contribute to the therapeutic effect.

In the present study unambiguous elucidation of the chemical structures of all relevant deferasirox metabolites formed in the rat was achieved. A key step towards this goal was the unambiguous identification of the C-3 and C-5 atoms in the ^{13}C–NMR spectra of the triazole ring, and subsequent assignment of all ^{13}C- and ^{1}H-signals of the phenol rings.

The disproportional increase of systemic exposure at the high dose level suggested that transport process(es), rather than biotransformation processes, are saturated. Excretion of deferasirox and metabolites occurred largely within 24 hours and was complete within 7 days. Residual traces of radioactivity were detected in the skin, kidney and liver. The biliary/fecal route of excretion was predominant. Further, deferasirox was marginally secreted with milk (3% of dose) and subsequently absorbed by the sucking pups. In these pups, the maximum concentration in highest exposed tissues (kidney cortex and liver) was approximately 8 times lower than in respective tissues of male rats serving as surrogate for dams. In the placental transfer study, the fetuses were also marginally exposed to the compound and/or its metabolites. From this finding it can be derived that human fetuses and infants will not be significantly exposed to deferasirox and/or its metabolites after oral administration to the mother.

The large proportion of dose that was excreted with the feces after po administration was predominantly the unchanged parent drug. This was due to: i) biliary elimination of deferasirox; ii) biliary elimination and intestinal hydrolysis of the glucuronide M3; iii) biliary elimination and dissociation of the Fe(deferasirox)$_2$ complex in the gut; and iv) incomplete intestinal absorption. The presence of large amounts of deferasirox in the intestine explains the observed reabsorption and enterohepatic recirculation, and the corresponding PK. It is important to note that orally administered deferasirox did not increase intestinal uptake of iron (Nick *et al*, 2000). This finding was supported by *in*

vitro data obtained with Caco-2 cells where transport of deferasirox but not the deferasirox–iron complex was observed.(Huang *et al*, 2006) (Novartis data on file)

Otherwise the fecal metabolite pattern was the same as phase I metabolites observed with liver microsomes *in vitro*. They were eliminated by conjugates with the bile, and were released from the conjugates in the gut by chemical and/or microbial hydrolysis.

In conclusion, deferasirox showed biopharmaceutical and metabolic properties that appear to be favorable for the intended oral therapeutic purpose of chelation and elimination of iron from the body.

Pharmacokinetics, metabolism and elimination of deferasirox differed strongly between Hanover-Wistar and TR^- rats, the latter being deficient in the anion transporter Mrp2. The observations in the TR^- rats confirm that the expression level of the transport protein Mrp2 has a marked impact on excretion and metabolism of deferasirox. The acyl glucuronide M3 is the major metabolite in normal rats, but only marginal amounts of M3 were excreted in TR^- rats. It could be hypothetized that this finding might be due to a deficiency of this strain in the specific glucuronyl transferase required. However, there is no data supporting this. It is far more likely that the acyl glucuronide M3 was formed in TR^- rats and that it is a good substrate of Mrp2. Though in the TR^- rats, any formed M3 could not be eliminated with the bile. In this situation M3 could be subject to esterase hydrolysis, liberating deferasirox, so that overall the formation of M3 appeared suppressed. Therefore metabolism and elimination were deviated to alternative processes which led to stable terminal metabolites *i.e.* O-sulfates and O-glucuronic acid conjugates of primary hydroxylated metabolites including M1 and M2. The conjugates were finally excreted via alternative transport systems and routes, with a marked shift towards the renal route. The major compensating metabolic process seems to be O-conjugation with sulfate.

Apart from the main metabolite M3, also unchanged deferasirox was excreted to a lower extent in TR^- rats. This observation indicates that the unchanged deferasirox is also a substrate of Mrp2.

From all results described in this paper, an overall picture emerges for the disposition of orally administered deferasirox in rats, as described schematically in Figure 9. This includes the following processes:

- The anion deferasirox can be eliminated from the liver into the bile. This process seems to be catalyzed, at least partly, by Mrp2.
- A major elimination process is the biotransformation of deferasirox to the anionic acyl glucuronide M3. M3 is a substrate of Mrp2, and is transported efficiently to the bile.

- In the gut, the acyl glucuronide M3 is unstable and will undergo hydrolysis to deferasirox, which will lead to some enterohepatic recirculation. The hydrolysis is probably due to microbial glucuronidases although spontaneous hydrolysis cannot be excluded. The lower proportion of unchanged deferasirox seen in plasma of TR^- rats may be due partly to diminished enterohepatic circulation resulting from reduced biliary excretion of both deferasirox and M3.
- Additional metabolites fomed are the primary hydroxylated derivatives M1, M2 and M4. These compounds undergo O-conjugation with sulfate and glucuronic acid. The resulting anionic O-conjugates (M7, M8, M9, M12, M13) are excreted both with bile and urine.
- If direct biliary elimination of deferasirox, and particularly if the key pathway to M3 is “suppressed” due to deficiency in mrp2, elimination by metabolism and hepatobiliary transport is slowed down, and the metabolism is shifted to other processes. Thus the basically minor metabolic processes compensate for the deficient key processes.
- The anionic O-conjugates formed as terminal metabolites can be eliminated to the bile, though to a similar degree, they are excreted by the alternative renal route. The latter implies that they are eliminated form the liver via basolateral transporter to the blood, and subsequently from the kidney to the urine. This results in an overall shift in the excretion routes and in the patterns of metabolites in the excreta.
- The transporter eliminating deferasirox and metabolites to the sinusoidal blood is unknown. However, a likely transport system is Mrp3. This carrier is localized at the basolateral membrane, is involved in the excretion of various organic anions from liver, and is known to be upregulated in case of mrp2-deficiency (König et al., 1999).

Overall, the herein reported studies have provided a comprehensive picture of the disposition of deferasirox in the rat and of the involved processes.

Acknowledgements

The authors wish to thank C Buffet, B Handschin, A Holler, B Inverardi, M Kuhn, F Marfil, S Osswald, J Pavel, D Pierroz, P Schnider, M Sütterlin, S Volz and A Wach for their excellent technical assistance and René Lattmann for synthesis of metabolites.

References

Bax A, Summers MF (1986) Proton and carbon-13 assignments from sensitivity-enhanced detection of heteronuclear multiple-bond connectivity by 2D multiple quantum NMR. *J Am Chem Soc* **108**: 2093-2094.

Begtrup M, Elguero J, Faure R (1988) Effect of N-substituents on the carbon-13 NMR parameters of azoles. *Magn Reson Chem* **26**:134-151.

Brittenham GM, Griffith PM, Nienhuis AW, McLaren CE, Young NS, Tucker EE, Allen CJ, Farrell DE, Harris JW (1994) Efficacy of deferoxamine in preventing complications of iron overload in patients with thalassemia major. *N Engl J Med* **331**:567-573.

Borst P, Balos E, and van de Wetering (2006) MRP2 and 3 in health and disease. *Cancer Lett* **234**:51-61.

Chan LM, Lowes S and Hirst BH (2004) The ABCs of drug transport in intestine and liver: efflux proteins limiting drug absorption and bioavailability. *Eur J Pharm Sci* **21**:25-51.

Cohen AR, Martin MB (2001) Iron chelation therapy in sickle cell disease. *Semin Hematol* **38** (1 Suppl 1):69-72.

Davies B and Morris T (1993) Physiological parameters in laboratory animals and humans. *Pharm Res* **10**:1093-1095

Dietrich CG, de Waart DR, Ottenhoff (2001) Mrp2-deficiency in the rat impairs biliary and intestinal excretion and influences metabolism and disposition of the food-derived carcinogen 2-amino-1-methyl-6-phenylimidazo[4,5-b]pyridine (PhIP). *Carcionogenesis* **22(5)**:805-811.

Gabutti V and Piga A (1996) Results of long-term iron-chelating therapy. *Acta Haematol* 95(1):26-36.

Hamaoka T (1990) Autoradiography of a new era replacing traditional X-ray film. *Cell Technol* 456-462.

Harkness JE (2001) What's your diagnosis? Hair loss in lactating rats. *Lab Animal* **30**: 21-22

Hershko C, Konijn AM, Nick HP, Breuer W, Cabantchik ZI, Link G (2001) ICL670A: a new synthetic oral chelator: evaluation in hypertransfused rats with selective radioiron probes of hepatocellular and reticuloendothelial iron stores and in iron-loaded rat heart cells in culture. *Blood* **97**:1115-1122.

Huang XP, Spino M, Thiessen JJ (2006) Transport kinetics of iron chelators and their chelates in Caco-2 cells. *Pharm Res* **23**:280-290.

Johnston RF, Pickett SC, Barker DL (1990) Autoradiography using storage phosphor technology. *Electrophoresis* **11**:355-360.

Kay LE, Keifer P, Saarinen T (1992) Pure absorption gradient enhanced heteronuclear single quantum correlation spectroscopy with improved sensitivity. *J Am Chem Soc* **114**:10663-10665.

Kim M-S, Liu DQ, Strauss JR, et al (2003) Metabolism and disposition of gemfibrozil in Wistar and muldrug resistance-assocoated protein 2-deficient TR$^-$ rats. *Xenobiotica* **33(19)**:1027-1044.

König J, Rost D, Cui Y, Keppler D (1999) Characterization of the human multidrug resistance protein isoform Mrp3 localized to the basolateral hepatocyte membrane. *Hepatology* **9(4)**:1156-1163.

Miyahara J (1989) Visualizing things never seen before - the imaging plate: a new radiation image sensor. *Chem Today* 29-36.

Nick H, Acklin P, Lattmann R, Buehlmayer P, Hauffe S, Schupp J, Alberti D (2003) Development of tridentate iron chelators: from desferrithiocin to ICL670. *Curr Med Chem* **10**: 1065-1076.

Nick HP, Acklin P, Faller B (2000) A new, potent, orally active iron chelator. In: Badman DG, Bergeron RJ, Brittenham GM (eds). Iron chelators: new development strategies. *Ponte Verde Beach: The Saratoga Group* 311-333.

Palmer III AG, Cavanagh J, Wright PE, Rance M (1991) Sensitivity improvement in proton-detected two-dimensional heteronuclear correlation NMR spectroscopy. *J Magn Reson* **93**:151-170

Olivieri NF (1999) The β-thalassemias. *N Engl J Med* **341**:99-109.

Olivieri NF, Brittenham GM (1997) Iron-chelating therapy and the treatment of thalassemia. *Blood* **89**:739-761.

Rath L, Hutchison M (1989) A new method of bile duct cannulation allowing bile collection and re-infusion in the conscious rat. *Lab Anim* **23**:163-168.

Rouan MC, Marfil F, Mangoni P, Sechaud R, Humbert H, Maurer G (2001) Determination of a new oral iron chelator, ICL670, and its iron complex in plasma by high-performance liquid chromatography and ultraviolet detection. *J Chromatogr B Biomed Sci Appl* **755**:203-213.

Schleucher J, Schwendinger M, Sattler M, Schmidt P, Schedletzky O, Glaser SJ, Sorensen OW, Griesinger C (1994) A general enhancement scheme in heteronuclear multidimensional NMR employing pulsed field gradients. *J Biomol NMR* **4**:301-306.

Schweitzer A, Fahr A, Niederberger W (1987) A simple method for the quantitation of 14C-whole-body autoradiograms. *Int J Rad Appl Instrum [A]* **38**:329-333.

Shigematsu A (1992) Bao-Bei, or the powerful technology, in science of whole-body metabolism. *Radioluminography* **3**:1-15.

Shionoya S (1992) Mechanistic approach toward photostimulated luminography. *Radioluminograpy* 1-15.

Shipkova M, Armstrong VW, Oellerich M, Wieland E (2003) Acyl glucuronide drug metabolites: toxicological and analytical implications. *Ther Drug Monit* **25**:1-16.

Steinhauser S, Heinz U, Bartholoma M, Weyhermuller T, Nick H, Hegetschweiler K (2004) Complex formation of ICL670 and related ligands with Fe III and Fe II. *Eur J Inorg Chem* **21**:4177-4192.

Ullberg S (1977) The technique of whole-body autoradiography: cryosectioning of large specimens. *In Science Tools, by Alvfeldt O (ed)* LDK-producter AB:Sweden: 2-29.

von Kienlin M, Moonene CTW, von der Toorn A, van Zijl PCM (1991) Rapid recording of solvent-suppressed 2D COSY spectra with inherent quadrature detection using pulsed field gradients. *J Magn Reson* **93**: 423-429.

Weiss HM, Fresneau M, Camenisch GP, Kretz O, Gross G (2006) In vitro blood distribution and plasma protein binding of the iron chelator deferasirox (ICL670) and its iron complex Fe-[ICL670]2, for rat, marmoset, rabbit, mouse, dog and human. *Drug Metab Dispos.* 34: 971-975.

Willker W, Leibfritz D, Kerssebaum R, Bermel W (1993) Gradient selection in inverse heteronuclear correlation spectroscopy. *Magn Reson Chem* **31**:287-292.

Footnotes

This study was supported by Novartis Pharma AG, Basel, Switzerland. This work was presented in part at the 51st American Society of Mass Spectrometry and Allied Topics meeting, Montreal, Canada, June 8–12, 2003.

[1] Current address of J.S.: Hoffmann-LaRoche, CH-4002 Basel, Switzerland

Figure legends

Figure 1. Chemical structures A) Deferasirox; B) Fe(deferasirox)$_2$ complex existing as anion form at physiological pH. The asterisk shows the position of the ^{14}C-label.

Figure 2. Plasma kinetics in Hanover-Wistar and in TR$^-$ rats. Concentrations of total radiolabeled components, deferasirox and its Fe-complex, [Fe (deferasirox)$_2$], in plasma of male rats after a) iv and b) po administration of 10 mg/kg of ^{14}C-deferasirox. Only the concentrations of total radiolabeled components in Hanover-Wistar rats were analyzed in individual animals. Deferasirox and Fe(deferasirox)$_2$ and concentrations of total radiolabeld components in TR$^-$ rats were analyzed in pools of three rats.

Figure 3. Selected whole-body autoradiograms. The whitest areas correspond to the highest concentrations of total radiolabeled components. a) male albino rat (lengthwise section through the side of the body) at 4 hours after a 100 mg/kg po dose of [^{14}C]deferasirox; b) male pigmented rat (lengthwise section through the side of the body) at 5 minutes after a 1 mg/kg iv dose of [^{14}C]deferasirox; c) female lactating dam (lengthwise section through the side of the body) at 24 hours after a 10 mg/kg po dose of [^{14}C]deferasirox; d) sucking pup (lengthwise section through the side of the body, 3-fold enlarged) at 8 hours after a 10 mg/kg po dose of [^{14}C]deferasirox to the lactating dam; e) pregnant rat (lengthwise section through the side of the body) at 2 hours after a 30 mg/kg po dose of [^{14}C]deferasirox.

Figure 4. Metabolite patterns in plasma, bile, feces and urine after iv dosing of 10 mg/kg iv in a Hanover-Wistar (a-d) and TR$^-$ rats (e-h). The feces were collected from rats that were not bile-cannulated and therefore demonstrate all metabolites eliminated through bile, after conjugate cleavage in the gut. a, e) 2-hour plasma; b, f) 0–48 hour bile; c, g) 0–48 hour feces; d, h) 0–48 hour urine.

Figure 5. Chemical structures of the major metabolites. Chemical structures of the major metabolites of deferasirox detected in plasma, urine, bile and feces of rats.

Figure 6. ^{1}H–NMR spectrum of deferasirox in DMSO-$d_{6.}$ a) Signal range; b) Aromatic region.

Figure 7. Important COSY, ROESY and HMBC correlations in deferasirox. The numbering of C-atoms from 1 to 24 differs from the common chemical numbering (cf. Figure 8) but was used for unambiguous denotation of C-atoms in NMR.

Figure 8. Schematic chemical structures of deferasirox and its metabolites, and of the metabolic pathways.

Figure 9. Proposed scheme for the disposition of deferasirox after peroral administration in normal rats and the role of Mrp2 therein. The substantial enterohepatic circulation is also included in this scheme.

Tables

Table 1

Pharmacokinetic parameters. Pharmacokinetic parameter in plasma after iv and po administration of [^{14}C]deferasirox and iv administration of [^{14}C]Fe(deferasirox)$_2$. (mean of n=3 rats each).

Compound administered	**[^{14}C]deferasirox**			**[^{14}C]Fe(deferasirox)$_2$**			**[^{14}C]deferasirox**			**[^{14}C]deferasirox**		
Dose, route	**10 mg/kg, iv**			**10 mg/kg, iv**			**10 mg/kg, po**			**100 mg/kg, po**		
	^{14}C	**DF**	**DF complex**	**^{14}C**	**DF**	**DF complex**	**^{14}C**	**DF**	**DF complex**	**^{14}C**	**DF**	**DF complex**
t_{max} [h]	0.08	0.08	1	0.08	0.08	0.08	0.5	0.5	2	8	1	4
C_{max} [µg/mL] [a]	22.9	25.3	2.03	91.7	1.57	90.0	3.18	2.65	0.49	56.4	52.6	6.11
C_0 [µg/mL] [a]	nc	29.1	nc	nc	128	nc	0	0	0	0	0	0
AUC [µg/mL•h] [a]	30.5	29.7	4.23	57.3	5.4	42.4	15.0	7.62	5.79	879	807	79.0
V_{ss} [L/kg]	nc	0.46	nc	nc	0.084	nc	nc	nc	nc	nc	nc	nc
CL [mL/kg/min]	nc	6.20	nc	nc	4.0	nc	nc	nc	nc	nc	nc	nc
MRT [h]	nc	1.25	nc	nc	0.35	nc	nc	nc	nc	nc	nc	nc
$t_{½}$ [h] [b]	nc	0.7	nc	nc	0.4	nc	nc	(0.5) [c]	nc	nc	nc	nc

DF: deferasirox, DF complex: Fe(deferasirox)$_2$

[a] to convert concentration data from mass units (µg/mL for defined compounds, µg-eq/mL for ^{14}C concentrations) to molar units (µmol/mL), divide by 373.4 (deferasirox) or 865.5 (Fe(deferasirox)$_2$); [b] For deferasirox after iv doing a time range of 5 minutes to 4 hours, for Fe(deferasirox)$_2$ of 5 minutes to 2 hours was considered; [c] For the initial elimination phase for defarasirox after po dosing, the time range from 1 to 2 hours was considered. This half life is only a descriptive estimate due to the low number of sampling time points; nc: not calculated

DMD Fast Forward. Published on September 5, 2008 as DOI: 10.1124/dmd.108.022962
This article has not been copyedited and formatted. The final version may differ from this version.

DMD #22962

Table 2

Deferasirox and metabolites in urine, bile and feces. Mean dose fractions excreted in non-cannulated and bile-cannulated rats following single oral 10 mg/kg doses of [^{14}C]deferasirox (0–48 hours; n=3). Under the given conditions of sample processing and chromatography, the iron complex dissociates and cannot be detected.

Compound/Metabolite	**Amount excreted [% dose]**						
	Non-cannulated rats			**Bile-cannulated rats**			
	Urine	**Feces**	**Total**	**Urine**	**Bile**	**Feces**	**Total**
M9	–	–	–	–	7.4	–	7.4
M8	0.7	–	0.7	0.7	5.4	–	6.1
M7	0.1	–	0.1	0.3	3.7	–	4.0
M6	1.4	–	1.4	0.7	2.8	–	3.5
M1	0.4	10.6	11.0	0.3	–	0.1	1.2
M2	–	6.2	6.2	–	–	0.1	0.1
M3	0.4	–	0.4	0.2	26.6	–	26.8
M4	1.9	5.2	7.1	1.6	2.8	0.1	4.5
M5	–	1.0	1.0	–	–	0.1	0.2
Deferasirox	0.2	49.7	49.9	0.1	7.7	14.9	22.7
Traces [a]	1.3	0.3	–	2.3	8.6	–	9.0
Not recovered [b]	0.6	20.2	21.8	1.0	4.2	5.6	10.8
Total Radioactivity [0–48 hours]	7.0	95.2	102.2	6.2	69.2	20.9	96.3

– not detected; [a]numerous metabolites <1% of dose; [b] not extracted and/or not recovered from HPLC

DMD Fast Forward. Published on September 5, 2008 as DOI: 10.1124/dmd.108.022962
This article has not been copyedited and formatted. The final version may differ from this version.

Table 3

Excretion of ^{14}C-radioactivity after iv and po administration of [^{14}C]deferasirox or [^{14}C]Fe(deferasirox)$_2$, as % of dose in Hanover-Wistar and TR$^-$ rats (mean of n=3; CV).

Compound and dosing	Time	Urine		Bile		Feces		Total	
	(h)	%	(CV%)	%	(CV%)	%	(CV%)	%	(CV%)
Hanover-Wistar rats									
[^{14}C]deferasirox 10 mg/kg, iv	0–24	6.59	(21)	na		61.9	(31)	68.5	(26)
	0–96	7.06	(19)	na		88.3	(6)	95.4	(6)
	0–168	7.18	(18)	na		89.0	(6)	96.1	(6)
[^{14}C]deferasirox 10 mg/kg, po	0–24	6.88	(18)	na		93.1	(1)	99.9	(1)
	0–96	7.05	(12)	na		95.2	(1)	102.2	(1)
	0–168	7.08	(12)	na		95.1	(1)	102.2	(1)
[^{14}C]deferasirox 10 mg/kg, po [a]	0–24	5.65	(21)	68.5	(14)	14.5	(54)	90.0	(5)
	0–72	6.29	(20)	69.3	(14)	21.5	(49)	97.2	(1)
[^{14}C]deferasirox 100 mg/kg, po	0–24	7.74	(20)	na		81.5	(2)	91.3	(1)
	0–96	10.6	(10)	na		90.0	(1)	100.6	(1)
	0–168	10.6	(10)	na		90.1	(1)	100.7	(1)
[^{14}C]Fe (deferasirox)$_2$ 10 mg/kg, iv	0–24	4.62	(20)	na		47.8	(31)	52.4	(27)
	0–96	5.2	(19)	na		89.	(2)	94.8	(2)

		9			5			
Mrp2-deficient TR$^-$ rats								
[^{14}C]deferasirox 10 mg/kg, iv	0–24	31.0	(13)	na	53.1	(9.9)	84.1	(10)
	0–72	33.1	(13)	na	58.6	(7.1)	91.7	(7.7)
[^{14}C]deferasirox 10 mg/kg, iv [a, b]	0-24	40.0		41.5	7.50		89.9	
	0-72	42.6		43.2	10.4		96.2	

[a] in bile duct-cannulated rats; [b] n=2; na, not collected or not analyzed

DMD Fast Forward. Published on September 5, 2008 as DOI: 10.1124/dmd.108.022962
This article has not been copyedited and formatted. The final version may differ from this version.

Table 4

Mass spectrometry data of deferasirox and its metabolites, and the chemical structure of deferasirox with common numbering of substructures as in Figure 8. The results for M1, M2, M4 and M5 were confirmed by analysis of synthetic reference compounds.

Compound / Metabolite	MW	Positive ion mode		Negative ion mode		Structure
		$[M+H]^+$	Key fragments	$[M-H]^-$	Key fragments	
Deferasirox	373	374		372	328 (M-H – CO_2) 252 (M-H – benzoic acid)	
M3	549	550	374 (M+H – glucuronic acid)	548	372 (M-H –glucuronic acid) 328 (M-H – glucuronic acid – CO_2)$^-$ 252 (M-H – glucuronic acid – benzoic acid)	Acyl glucuronide
M3'	549	550				Isomers of M3 by acyl migration
M1	389	390		388	344 (M-H – CO2) 268 (M-H – benzoic acid)	5-OH
M2	389	390				3-OH
M4	389	390		388	344 (M-H – CO2) 268 (M-H – benzoic acid)	5'-OH
M5	389	390		*b*		3'-OH
M9	565	566	390 (M+H – glucuronic acid)	564	344 (M-H – glucuronic acid)	5-O-glucuronide
M7	469	470	390 (M+H – sulfate)	468	388 (M-H – sulfate) 344 (M-H – sulfate – CO_2) 268 (M-H – sulfate – benzoic acid)	5-O-sulfate
M8	469	470	390 (M+H – sulfate)	468	388 (M-H – sulfate) 344 (M-H – sulfate – CO_2) 268 (M-H – sulfate – benzoic acid)	3-O-sulfate
M11	565	566	390 (M+H – glucuronic acid)	564	388 (M-H – glucuronic acid) 344 (M-H – glucuronic acid – CO_2)$^-$ 268 (M-H – glucuronic acid – benzoic acid)	3'-O-glucuronide
M6	549	550	374 (M+H – glucuronic acid)	548	372 (M-H – glucuronic acid) 328 (M-H – glucuronic acid – CO_2)	2-O-glucuronide
M13	453	454	374 (M+H – sulfate)	452	372 (M-H – sulfate) 328 (M-H – sulfate – CO_2) 252 (M-H – sulfate – benzoic acid)	2- or 2'-O-sulfate
M12	629	630	550 (M+H – sulfate) 374 (M+H – glucuronic acid – sulfate)	628	548 (M-H – sulfate) 372 (M-H – glucuronic acid – sulfate) 328 (M-H – glucuronic acid – sulfate – CO_2)	O-glucuronide and O-sulfate [a]

[a] position of glucuronic acid and sulfate not identified, [b] no signals in negative ion mode due to insufficient sensitivity

DMD Fast Forward. Published on September 5, 2008 as DOI: 10.1124/dmd.108.022962
This article has not been copyedited and formatted. The final version may differ from this version.

DMD #22962

Table 5

NMR data of deferasirox. The C atoms are listed in descending order of the ^{13}C-shifts. For NMR, the carbon atoms were numbered systematically from C-1 to C-24, as shown in Figure 7.

C-atom	Atom	^{13}C-shift [ppm] [a]	Carbon multiplicity from ^{13}C- and 2D ^{1}H,^{13}C-COSY (HSQC) spectrum	^{1}H-shift [ppm] [a] and ^{1}H,^{13}C-COSY (HSQC) [c] correlations	^{1}H multi-plicity	^{1}H-^{1}H COSY correlations [b]	^{1}H,^{13}C long range correlations from HMBC spectrum, ^{1}H-shifts [d]
24	C	166.4	C_q				7.98
3	C	159.9	C_q				8.04
13	C	156.3	C_q				10.78/8.04/7.37
19	C	155.2	C_q				7.39
5	C	152.0	C_q				7.54
6	C	141.1	C_q				7.98
21	C	132.5	CH	7.39	t	6.98/6.86	
15	C	131.4	CH	7.37	td	7.00/7.02	
23	C	131.0	CH	7.54	dd	6.98	
9	C	130.6	C_q				7.55
8/10	C	130.3	CH	7.98	dm	7.55	
17	C	126.7	CH	8.04	dd	7.00	
7/11	C	123.3	CH	7.55	dm	7.98	
16	C	119.7	CH	7.00	t	8.04/7.37	
22	C	119.4	CH	6.98	t	7.54/7.39	
14	C	117.0	CH	7.02	d	7.37	10.78
20	C	116.1	CH	6.86	d	7.39	
18	C	114.4	C_q				6.86
12	C	113.6	C_q				10.78
13-OH				10.78	s		
19-OH				10.04	sbr		
COOH				13.19	sbr		

[a] chemical shift reference: internal to the middle line of the DMSO-d_6 NMR solvent signal: ^{1}H: δ = 2.500 ppm; ^{13}C: δ = 39.52 ppm; concentration: 30 mg in 0.7 ml DMSO-d_6; Abbreviations: ^{1}H multiplicity: s, singlet; d, doublet; t, triplet; q, quartet; br, broad

[b] 1H,^{1}H-COSY: Homonuclear Correlated spectroscopy. Magnitude experiment with z gradient (Hurd,1990; Von Kienlin et al., 1991)

[c] ^{1}H,^{13}C-COSY HSQC experiment: Heteronuclear Correlated spectroscopy. Heteronuclear single quantum coherence experiment with ^{1}H detection, z-gradient and echo-antiecho sensitivity enhancement (Palmer III et al., 1991; Kay et al., 1992; Schleucher, 1994):

[d] long-range ^{1}H,^{13}C-COSY, HMBC experiment: Heteronuclear Correlated spectroscopy. Heteronuclear multiple bond correlation experiment with ^{1}H detection and z-gradient (Bax et al., 1986; Willker et al., 1993).

DMD Fast Forward. Published on September 5, 2008 as DOI: 10.1124/dmd.108.022962
This article has not been copyedited and formatted. The final version may differ from this version.

Table 6

^{1}H–NMR data of deferasirox and its metabolites. Carbon atoms were numbered systematically from C-1 to C-24, as shown in Figure 7. Specific ^{1}H–NMR signals showing characteristic shifts compared with deferasirox are in bold print. The OH substituents in the metabolites caused the typical high field shifts of ^{1}H-signals in the ortho and para position. Specific couplings indicated the presence or absence of specific regio isomers. The results for M1, M2 and M4 were confirmed by analysis of synthetic reference compounds.

C-atom	Deferasirox		M1		M2		M3		M4	
	^{1}H-shift [ppm]	^{1}H-multiplicity	^{1}H-shift [ppm]	^{1}H-multiplicity	^{1}H-shift [ppm]	^{1}H-multiplicity	^{1}H-shift [ppm]	^{1}H-multiplicity	^{1}H-shift [ppm]	^{1}H-multiplicity
8/10	7.98	dm	7.91	dm	7.92	dm	**8.09**	dm	7.93	dm
7/11	7.55	dm	7.42	dm	7.44	dm	7.60	dm	7.46	dm
23	7.54	dd 8.0/1.8	7.48	dd 7.6/1.7	7.49	dd large/small [a]	7.58	dd large/small	**6.86**	**d small** [b]
22	6.98	t large	6.94	t large	6.95	t large	6.99	t large	**–-**	
21	7.39	td large/small	7.36	td large/small	7.37	td large/small	7.39	td large/small	**6.79**	dd large/small
20	6.86	d 8.0	6.86	d 8.0	6.86	d 8.0	6.84	d large	**6.68**	d large
17	8.04	dd 8.0/1.6	**7.45**	**d 2.8** [b]	**7.48**	dd large/small [a]	8.05	dd large/small	8.03	dd large/small
16	7.00	t	**–-**		**6.79**	**t large** [c]	7.00	t large	6.99	t large
15	7.37	td 8.0/1.5	**6.78**	dd 8.8/2.8	**6.88**	dd large/small	7.37	td large/small	7.36	t large
14	7.02	d 8.0	**6.83**	d 8.8	**–**		7.02	d large	7.01	d large
OH	10.78 (13-OH)	s	**10.22**	s	10.77	sbr	10.76 (13-OH)	sbr	10.86	s
OH	10.04 (19-OH)	sbr	10.13	sbr	10.12	sbr	10.01 (19-OH)	sbr	**9.33**	sbr
OH			9.09	sbr	9.11	sbr	–		9.16	sbr
COOH	13.19	sbr	Not visible		Not visible		12.87	sbr		Not visible
H-1'							5.62	d large		
H-3'/4'/5'							under water signal			
H-5'							3.85	d large		

[a] signal overlapping; chemical shift reference: internal to the middle line of the DMSO-d_6 NMR solvent signal: ^{1}H: δ = 3.300 ppm; [b] meta coupling of an "isolated" H; rules out regio isomers with 3 neighbored H; [c] triplet indicates 2 vicinal H; rules out regio isomers with an "isolated" H; Abbreviations: ^{1}H multiplicity: s, singlet; d, dublet; t, triplet; q, quartet; br, broad; m, multiplet; large: ^{1}H,^{1}H coupling constant is about 7–8 Hz; small: ^{1}H,^{1}H coupling constant is about 1–3 Hz

DMD Fast Forward. Published on September 5, 2008 as DOI: 10.1124/dmd.108.022962

Figure 1

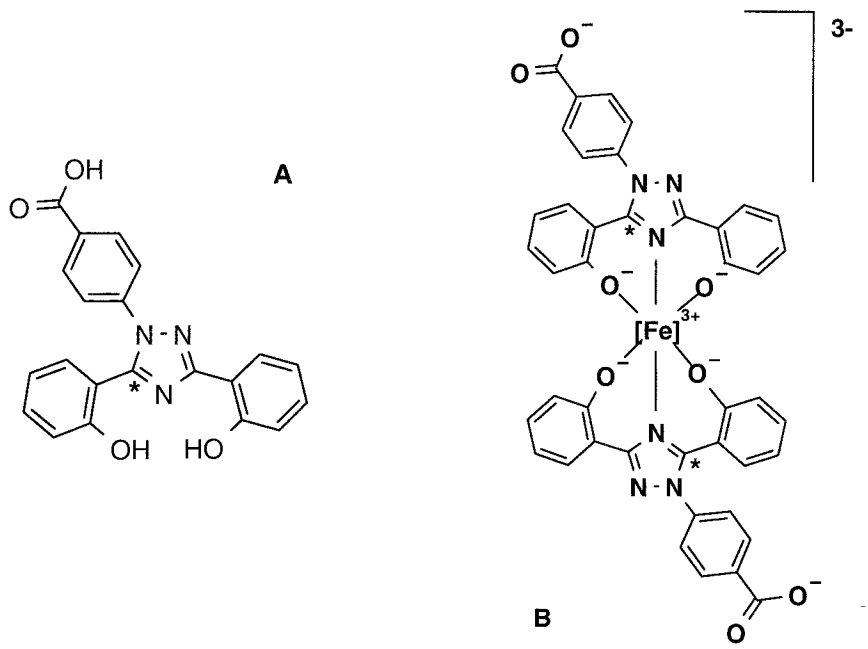

DMD Fast Forward. Published on September 5, 2008 as DOI: 10.1124/dmd.108.022962
This article has not been copyedited and formatted. The final version may differ from this version.

Figure 2

a

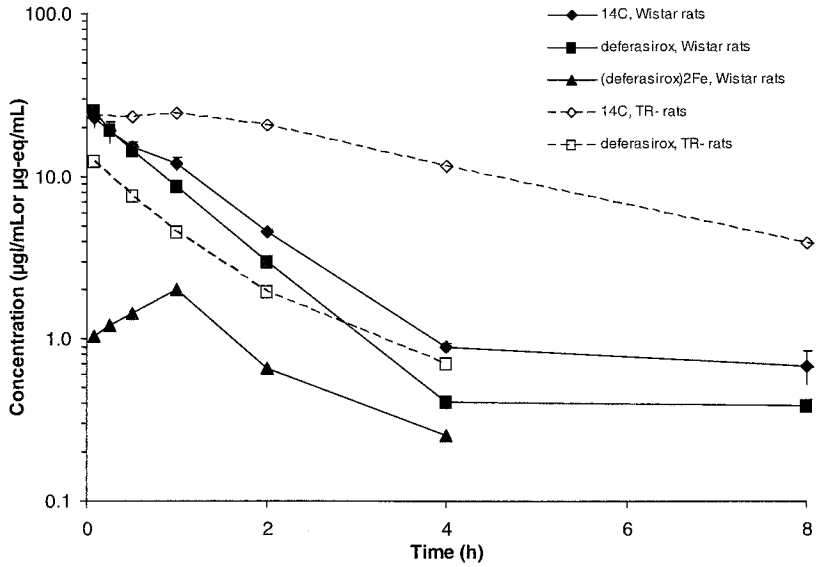

b

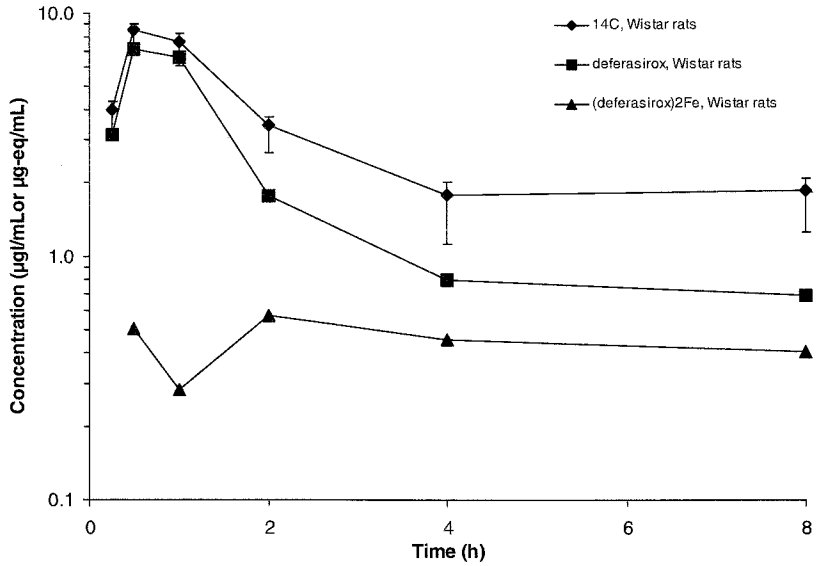

Figure 3

a

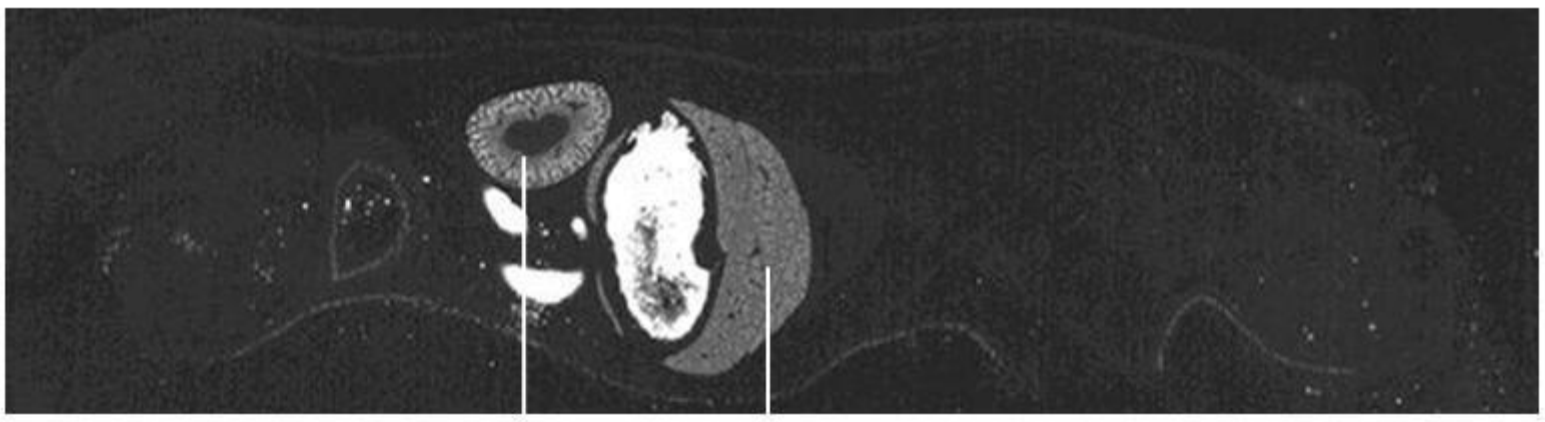

b

c

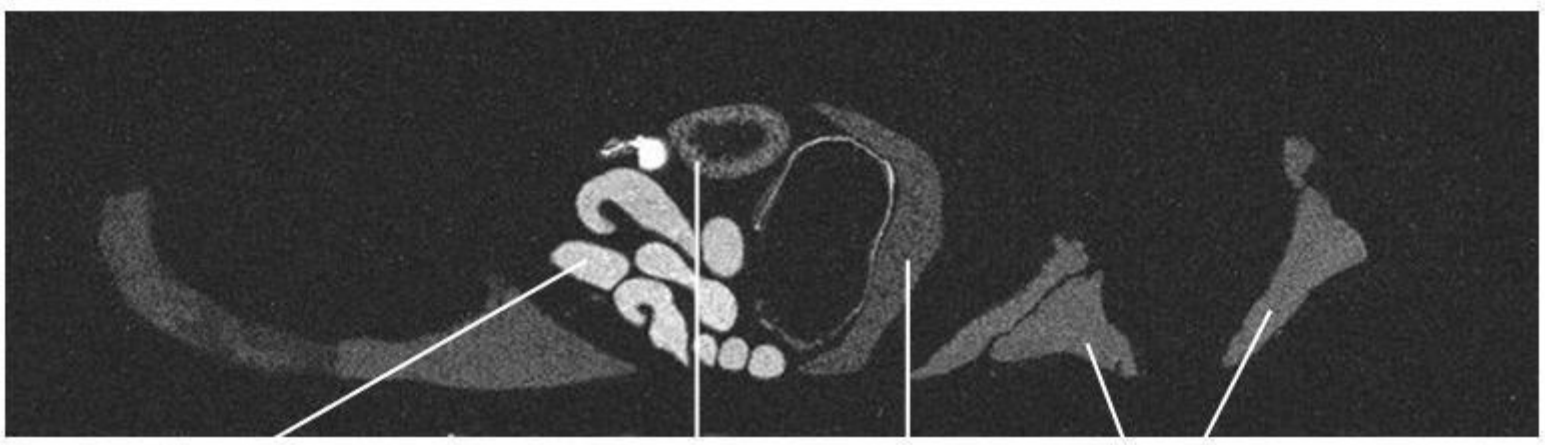

d

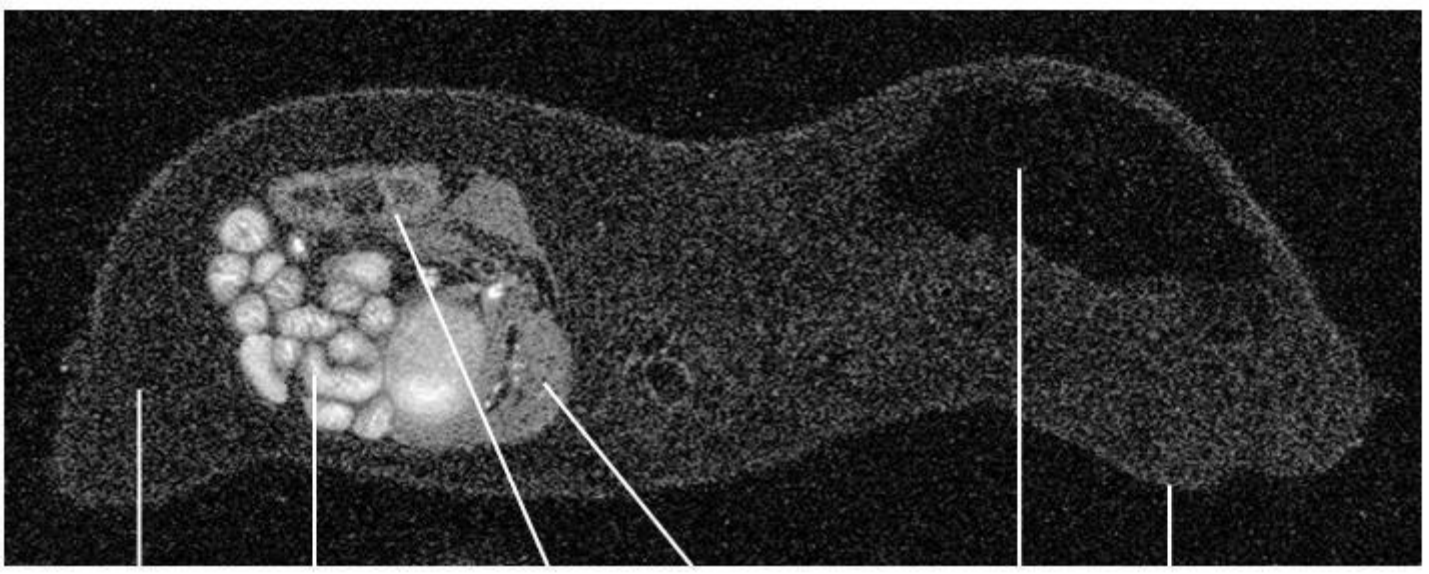

e

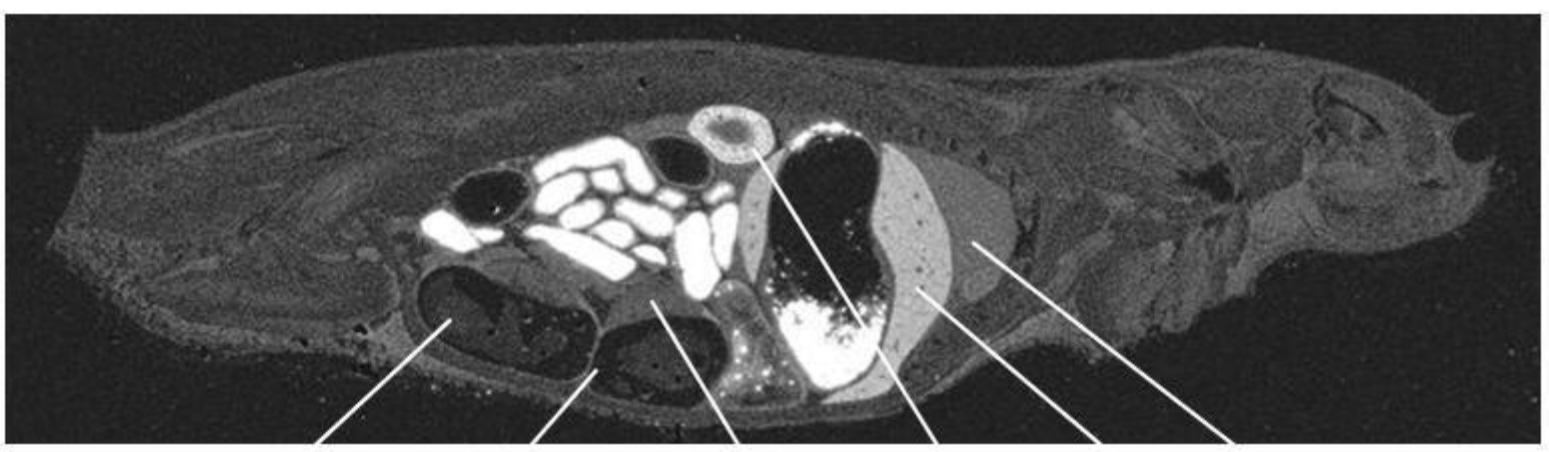

Figure 4

DMD Fast Forward. Published on September 5, 2008 as DOI: 10.1124/dmd.108.022962
This article has not been copyedited and formatted. The final version may differ from this version.

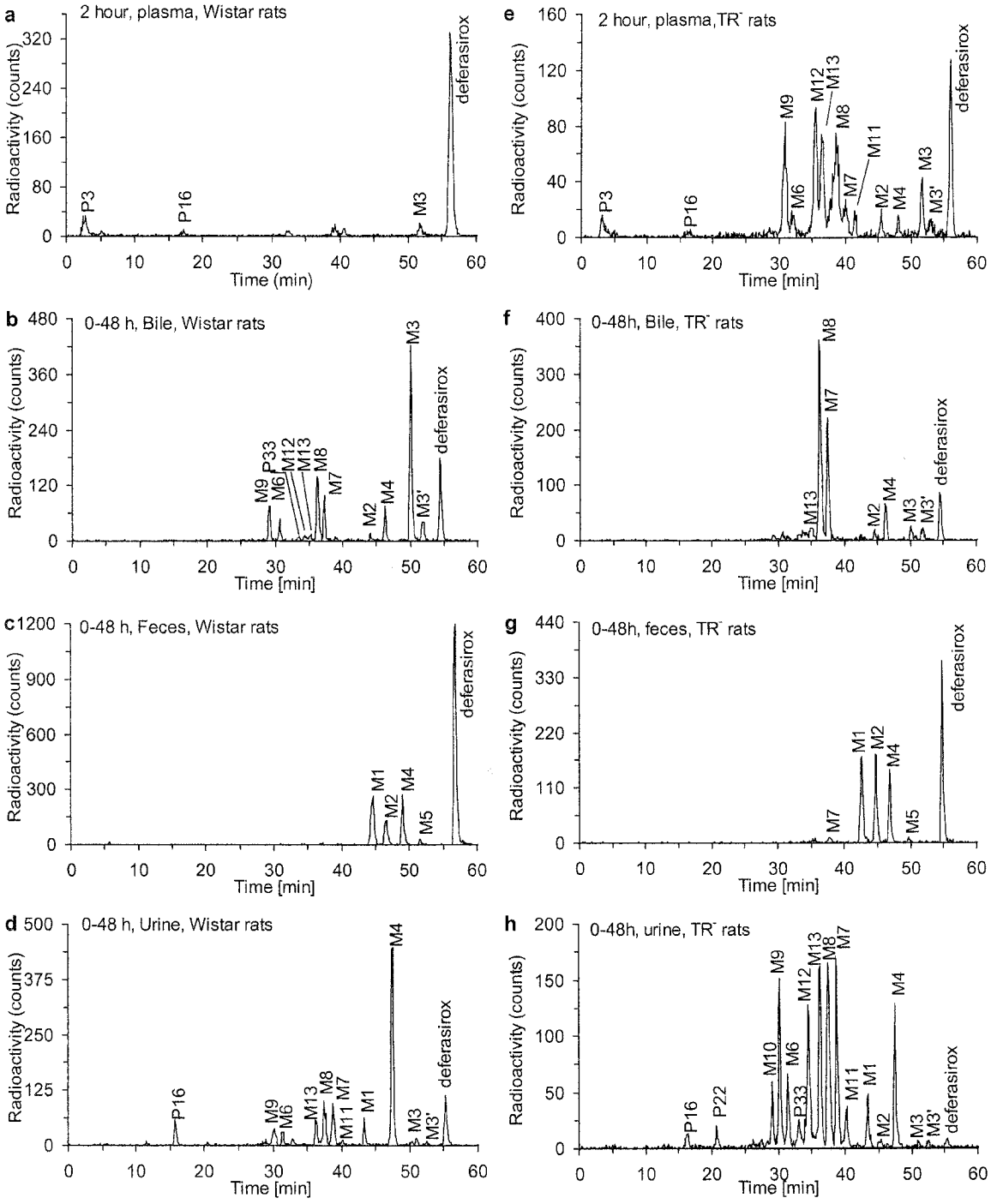

DMD Fast Forward. Published on September 5, 2008 as DOI: 10.1124/dmd.108.022962
This article has not been copyedited and formatted. The final version may differ from this version.

Figure 5

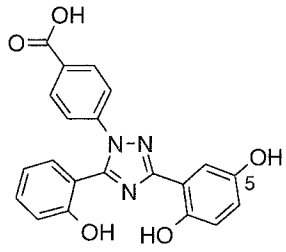

M1 (m.w. 390)

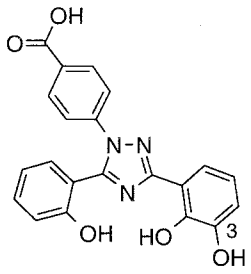

M2 (390)

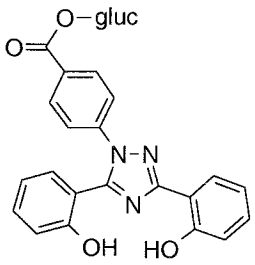

M3 (550)

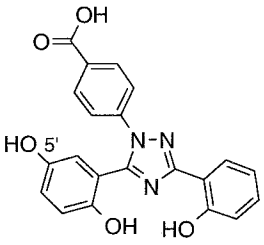

M4 (390)

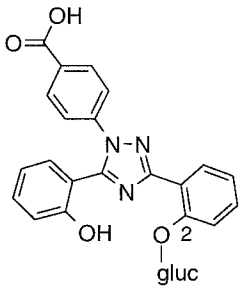

M6 (550)

DMD Fast Forward. Published on September 5, 2008 as DOI: 10.1124/dmd.108.022962

Figure 6

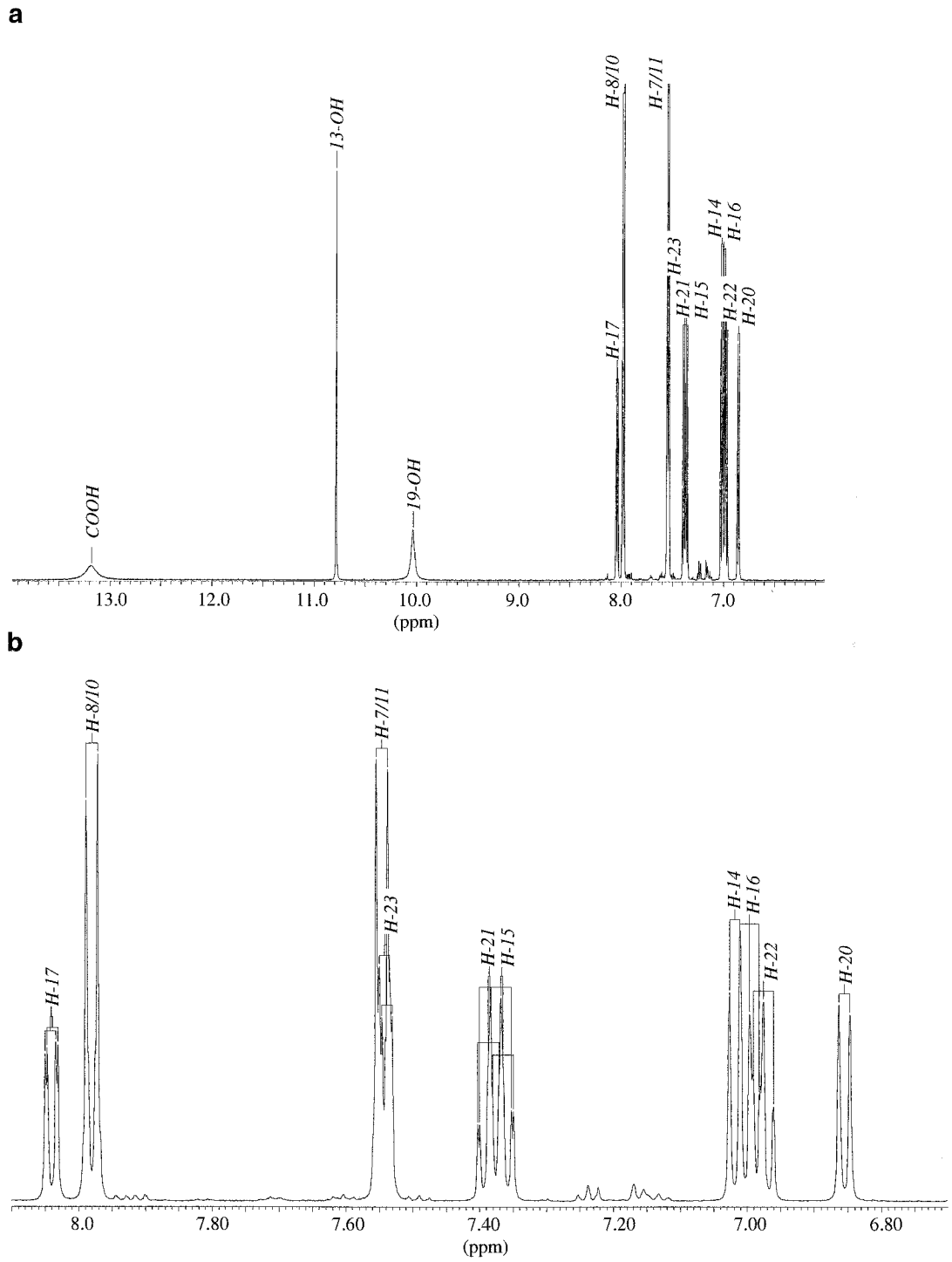

DMD Fast Forward. Published on September 5, 2008 as DOI: 10.1124/dmd.108.022962

Figure 7

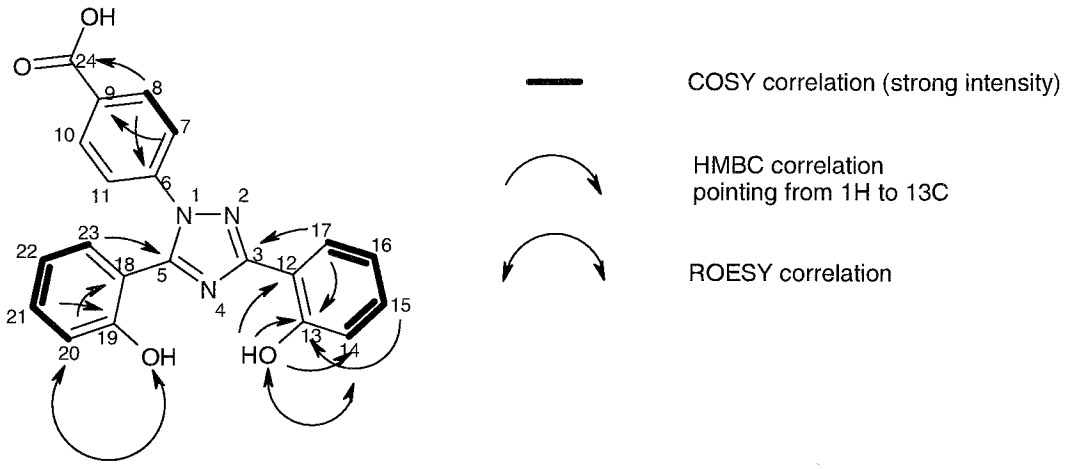

DMD Fast Forward. Published on September 5, 2008 as DOI: 10.1124/dmd.108.022962
This article has not been copyedited and formatted. The final version may differ from this version.

Figure 8

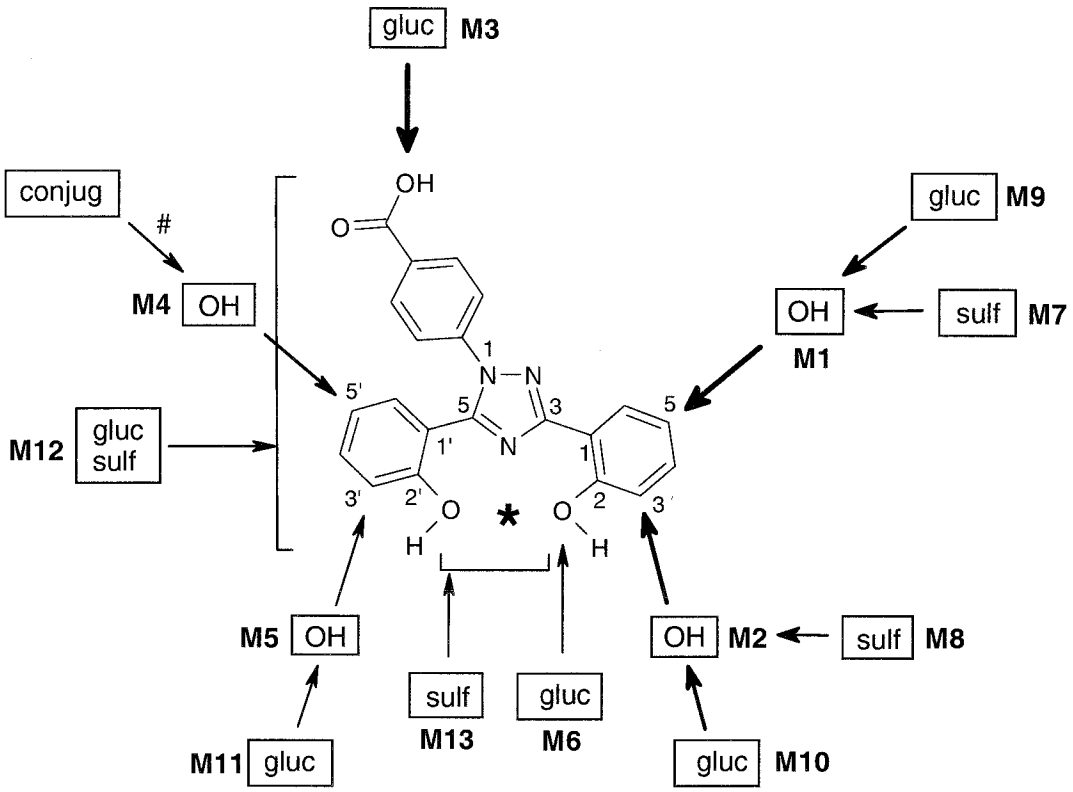

OH	hydroxylation	gluc	O-glucuronidation
sulf	O-sulfation	conjug	glucuronidation and/or sulfation
*	position of Fe^{3+} ion in complex	#	hypothetical

Figure 9